N 72 - 13582

NASA TECHNICAL MEMORANDUM

NASA TM X-64628

CASE FILE COPY

ANGULAR MOMENTUM DESATURATION FOR SKYLAB USING GRAVITY GRADIENT TORQUES

By Hans F. Kennel
Astrionics Laboratory

December 7, 1971

NASA

George C. Marshall Space Flight Center
Marshall Space Flight Center, Alabama

MSFC - Form 3190 (Rev June 1971)

TECHNICAL REPORT STANDARD TITLE PAGE

1. REPORT NO.	2. GOVERNMENT ACCESSION NO.	3. RECIPIENT'S CATALOG NO.
TM X-64628		

4. TITLE AND SUBTITLE	5. REPORT DATE / 6. PERFORMING ORGANIZATION CODE
Angular Momentum Desaturation for Skylab Using Gravity Gradient Torques	December 7, 1971
7. AUTHOR (S) Hans F. Kennel	8. PERFORMING ORGANIZATION REPORT #
9. PERFORMING ORGANIZATION NAME AND ADDRESS George C. Marshall Space Flight Center, Marshall Space Flight Center, Alabama 35812	10. WORK UNIT NO. / 11. CONTRACT OR GRANT NO.
12. SPONSORING AGENCY NAME AND ADDRESS National Aeronautics and Space Administration, Washington, D. C. 20546	13. TYPE OF REPORT & PERIOD COVERED: Technical Memorandum / 14. SPONSORING AGENCY CODE

15. SUPPLEMENTARY NOTES

Prepared by the Astrionics Laboratory, Science and Engineering

16. ABSTRACT

An angular momentum desaturation method for momentum exchange devices of orbiting spacecraft is described. The specific application of the method is to the Skylab which contains three double-gimbaled control moment gyros for precise attitude control and maneuvering. It is assumed that the attitude reference is inertially fixed and that two of the vehicle principal moments of inertia are much larger than the third. Gravity gradient torques and resultant angular momentum accumulation are developed for small deviations from the reference. The assumed moment-of-inertia distribution allows desaturation about all axes with only two attitude angles each for the two axes with large moments of inertia. The necessary desaturation maneuvers can be decoupled for a special set of orbital coordinates. All maneuvers are made during the night portion of the orbit, and the percentage utilized for desaturation is selectable. Expressions for the attitude angle commands are developed assuming infinite vehicle rates. The effect of finite rates introduces an efficiency into the desaturation. Expressions for this efficiency are developed and means for compensation are treated. Arbitrary misalignments between geometric vehicle axes and principal moment-of-inertia axes are permissible. An angle bias about the sun line minimizes the angular momentum accumulation about the sun line projection into the orbital plane. Adaptive desaturation maneuver limiting consistent with the available maneuver momentum is included.

17. KEY WORDS	18. DISTRIBUTION STATEMENT
Angular Momentum Desaturation Control Moment Gyro Control Law Space Station	Unclassified-unlimited Hans F. Kennel

19. SECURITY CLASSIF. (of this report)	20. SECURITY CLASSIF. (of this page)	21. NO. OF PAGES	22. PRICE
Unclassified	Unclassified	62	$3.00

MSFC - Form 3292 (May 1969)

TABLE OF CONTENTS

	Page
SUMMARY	1
INTRODUCTION	1
GRAVITY GRADIENT TORQUE	2
MOMENTUM DESATURATION METHOD	4
General	4
Desaturation Angle Generation	5
Angular Momentum Sampling	13
Desaturation Command Generation	16
APPENDIX A. DEFINITIONS OF SKYLAB COORDINATE SYSTEMS AND ANGLES	19
APPENDIX B. DERIVATION OF GRAVITY GRADIENT TORQUE	21
APPENDIX C. COEFFICIENT EVALUATION	25
APPENDIX D. DESATURATION MANEUVER EFFICIENCIES	27
APPENDIX E. ORBITAL ELEVATION OF PRINCIPAL z_p AXIS; NOMINAL ROTATION υ_{zg} ABOUT THE SUN LINE; AND GRAVITY GRADIENT TORQUE PHASE SHIFT η_{tm}	31
APPENDIX F. MANEUVER MOMENTUM PREDICTION AND ADAPTIVE ANGLE COMMAND LIMITING	34
APPENDIX G. CYCLE MOMENTUM COMPONENTS	44
APPENDIX H. SAMPLED DATA SYSTEM	48
REFERENCES	50

LIST OF ILLUSTRATIONS

Figure	Title	Page
1.	Angular momentum accumulation about the x_{pr} axis	4
2.	Typical cyclic angular momentum	5
3.	Desaturation angle profiles	8
4.	Relative desaturation capacity about orbital y axis	10
5.	Typical CMG momentum profile	14
6.	Orbital angular momentum sampling points	15
F1.	Checkpoints for maneuver momentum	36
F2.	Orbital z versus orbital y momentum	37
F3.	$\Delta\rho$-generation	38
F4.	Exact $\Delta\rho/(\rho/2)$ versus λ_4	39
F5.	Approximate $\Delta\rho/(\rho/2)$ versus λ_4	40

DEFINITION OF SYMBOLS

a_{ij}	coefficients [equation (6)], (i = 1, 2, 3; j = 1, 2, 3)
a_y, a_z	orbital coefficients [equation (12)]
A_i	[1/(Nms)] coefficients [equations (6) and (17)] (i = 1, 2, 3, 4)
A_{ij}	coefficients [equation (5)] (i = 1, 2, 3; j = 1, 2, 3)
c	cosine (with Greek symbol immediately following)
[c], c_{ij}	transformation matrix from CS X_{or} to CS X_{pr} and its elements (i = 1, 2, 3; j = 1, 2, 3)
E_i	desaturation efficiencies (i = x, y, z)
[E]	identity matrix
h	[Nms] z-transform of H
$\underline{H}_a$	[Nms] average momentum at noon
$\underline{H}_b$	[Nms] desired momentum bias
$\underline{H}_c$	[Nms] cosine amplitude of cyclic momentum (from samples)
$\underline{H}_d$	[Nms] desaturation momentum command
$\underline{H}_g$	[Nms] momentum caused by gravity gradient torques
$\underline{H}_{gc}$	[Nms] cyclic momentum portion of $\underline{H}_g$ (predicted)
$\underline{H}_{gy}$	[Nms] cosine amplitude of cyclic momentum (along y_{or}, predicted)
$\underline{H}_{gz}$	[Nms] sine amplitude of cyclic momentum (predicted)
$\underline{H}_k$	[Nms] momentum accumulation per orbit caused by constant torques
$\underline{H}_{man}$	[Nms] maneuver momentum

DEFINITION OF SYMBOLS (Continued)

$\underline{H}_s$	[Nms] sine amplitude of cyclic momentum (from samples)
$\underline{H}_t$	[Nms] total vehicle/CMG momentum
$\underline{\Sigma H}_a$	[Nms] intermediate quantity for desaturation command generation
$\underline{\Sigma H}_{mib}$	[Nms] sum of MIB momentum since sample at t_2
[I]	[kg m²] moment-of-inertia matrix
$[I_p]$	[kg m²] principal moment-of-inertia matrix
I_i	[kg m²] principal moments of inertia (i = x, y, z)
ΔI_i	[kg m²] differences of principal moments of inertia (i = x, y, z)
[K], K_{ij}	transformation matrix from geometric vehicle CS X_v to principal CS X_p and its elements (i = 1, 2, 3; j = 1, 2, 3)
K_n, K_{n-1}	gain constants
n, n-1	subscripts indicating present (n) or past (n-1) orbit
$\underline{r}$	unit vector along the direction of the gravity gradient
s	sine (when followed by Greek symbol)
t	tangent (when followed by Greek symbol)
$\underline{T}_g$	[Nm] gravity gradient torque
$\underline{T}_{gc}$	[Nm] cyclic portion of gravity gradient torque
$\underline{T}_{gd}$	[Nm] gravity gradient torque used for desaturation
$\underline{T}_{gn}$	[Nm] nominal gravity gradient torque

$\left.\begin{matrix} x_{ij} \\ y_{ij} \\ z_{ij} \end{matrix}\right\}$	coordinate axes of CS X_{ij} (Appendix A)
$\underline{X}_{ij}$	coordinate system as indicated by the subscripts (Appendix A)
α	dummy integration variable
$[\alpha_x]$	$\begin{bmatrix} 1 & 0 & 0 \\ 0 & c\alpha_x & s\alpha_x \\ 0 & -s\alpha_x & c\alpha_x \end{bmatrix}$ where α can be any Greek symbol
$[\alpha_y]$	$\begin{bmatrix} c\alpha_y & 0 & -s\alpha_y \\ 0 & 1 & 0 \\ s\alpha_y & 0 & c\alpha_y \end{bmatrix}$ where α can be any Greek symbol
$[\alpha_z]$	$\begin{bmatrix} c\alpha_z & s\alpha_z & 0 \\ -s\alpha_z & c\alpha_z & 0 \\ 0 & 0 & 1 \end{bmatrix}$ where α can be any Greek symbol
$\epsilon_i, \Delta\epsilon_i$	[rad] desaturation angles (in CS X_{pr})
$\epsilon_{i1}, \epsilon_{i2}$	[rad] desaturation angles (in CS X_{vr})
$\epsilon_i', \Delta\epsilon_i'$	[Nms] normalized desaturation angles
η	[rad] elevation of principal z_{pr} axis with respect to orbital plane
η_t	[rad] timing angle with respect to orbital midnight
η_{td}	[rad] timing angle with respect to orbital desaturation midnight
η_{tm}	[rad] difference between η_{td} and η_t

DEFINITION OF SYMBOLS (Concluded)

η_x	[rad] elevation of reference z_r axis with respect to orbital plane
η_{xp}	[rad] principal axes transformation angle (Appendix A)
η_y	[rad] angle between CS X_o and CS X_{or}
λ, λ_i	ratios of available to commanded maneuver momentum
υ_z	[rad] angle between CS X_r and CS X_{vr}
$\Delta\upsilon_z$	[rad] commanded change of υ_z at end of desaturation interval
υ_{ze}	[rad] elevation of the x_{pr} axis with respect to orbital plane
υ_{zg}	[rad] see Appendix A for definition
υ_{zp}	[rad] see Appendix A for definition
ρ	[rad] orbital half angle used for desaturation
ρ'	[rad] variable orbital half angle used for efficiency determination
$\Delta\rho$	[rad] shortening of desaturation interval to insure error-free attitude closing
$\underline{\phi}_e$	[rad] attitude deviation (either commanded or error)
Ω	[rad/s] orbital angular velocity

TECHNICAL MEMORANDUM X-64628

ANGULAR MOMENTUM DESATURATION FOR SKYLAB USING GRAVITY GRADIENT TORQUES

SUMMARY

The angular momentum desaturation method for the Skylab is presented. This method utilizes the gravity gradient torques and therefore minimizes the necessity for mass expulsion by the thruster attitude control system (TACS). The desaturation method requires maneuvers about the two principal axes of large inertia. The percentage of the orbit used for desaturation is selectable. An arbitrary misalignment between the axes of principal moments of inertia and the geometric vehicle axes is permissible. An angle bias about the sun line minimizes the momentum accumulation in the orbital plane.

This report is an extensive revision of Reference 1. The desaturation scheme has been expanded to include arbitrary principal moment-of-inertia axes misalignment, adaptive maneuver limiting according to the available maneuver momentum, and reduction of the third-order sampled data system to a second order.

INTRODUCTION

The Skylab Apollo Telescope Mount (ATM) experiments require that the solar instruments remain inertially fixed (sun-oriented) during the day portion of the orbit. Gravity gradient, aerodynamic, venting, and other external torques acting on the vehicle during this time must be absorbed by an angular momentum storage device; in this instance, a system of three double-gimbaled control moment gyros (CMG's) [2, 3, 4, 5]. Portions of the disturbance torques are noncyclic and tend to saturate the CMG system, which has a limited momentum storage capacity. A method for momentum desaturation that does not require mass expulsion is desired. The gravity gradient torques acting on Skylab are developed for small deviations from the sun-oriented reference coordinate system. These equations are used to show that maneuvers about the two axes of large moments of inertia are sufficient to desaturate the accumulated momenta about all axes. All attitude maneuvers for desaturation are made during the night portion of the orbit (unless an insufficient night portion is available, where part of the daylight portion is used), and the percentage of the orbit utilized for desaturation is selectable. Expressions for the desaturation angle commands are developed assuming infinite angular vehicle rates. The effect of finite rates then introduces an efficiency, which is calculated and compensated for by a change in the commanded maneuver. An arbitrary misalignment between the principal moment-of-inertia axes and the geometric axes of the vehicle is acceptable. An angle bias about the sun line allows the minimization of the momentum component along the projection of the z_p axis into the orbital plane (see Appendix A for coordinate system definitions, etc.).

The desaturation angles have been assumed to be small enough to make small angle approximations valid which allows the principle of superposition and also allows the treatment of the angles as if they were vectors.

To avoid endless repetition in the following discussion, "momentum" is used for "angular momentum," "desaturation" is used for "angular momentum desaturation," and "vehicle axes" means "geometric vehicle axes."

GRAVITY GRADIENT TORQUE

The gravity gradient torque acting on the vehicle can be expressed as [6]

$$\underline{T}_g = 3\,\Omega^2 [\tilde{r}]\ [I]\ \underline{r} \tag{1}$$

when the vehicle is in a circular orbit (which is assumed in the further development); $[I]$ is the vehicle inertia matrix, Ω is the orbital rate, $\underline{r}$ is a unit vector parallel to the radius vector from the earth center to the vehicle center of mass, and $[\tilde{r}]$ is defined as

$$[\tilde{r}] = \begin{bmatrix} 0 & -r_z & +r_y \\ +r_z & 0 & -r_x \\ -r_y & +r_x & 0 \end{bmatrix}$$

When the torque is expressed in the principal reference system, PR (see Appendix A for definitions), when $[I_p]$ is the principal moment-of-inertia matrix, and when $[\epsilon]$ is the transformation from the PR system to the P system, the equation (1) becomes

$$\underline{T}_g = 3\Omega^2 [\tilde{r}_{pr}][\epsilon]^T\ [I_p]\ [\epsilon]\ \underline{r}_{pr} \tag{2}$$

or

$$\underline{T}_g = \underline{T}_{gn} + \underline{T}_{gd} \tag{3}$$

with

$$\underline{T}_{gn} = \frac{3}{2}\,\Omega^2 \begin{bmatrix} \frac{1}{2}\ s2\eta\ (1 + c2\eta_{td})\,\Delta I_x \\ c\eta\ s2\eta_{td}\,\Delta I_y \\ s\eta\ s2\eta_{td}\,\Delta I_z \end{bmatrix} \tag{4}$$

$$\underline{T}_{gd} = \frac{3}{2}\,\Omega^2 \begin{bmatrix} +A_{11} & +A_{12} & +A_{13} \\ -A_{12} & +A_{22} & +A_{23} \\ -A_{13} & -A_{23} & +A_{33} \end{bmatrix} \begin{bmatrix} \Delta I_x\,\epsilon_x \\ \Delta I_y\,\epsilon_y \\ \Delta I_z\,\epsilon_z \end{bmatrix} \tag{5}$$

$$\Delta I_x = I_z - I_y$$

$$\Delta I_y = I_x - I_z$$

$$\Delta I_z = I_y - I_x$$

$$A_{11} = +c2\eta\ (1 + c2\eta_{td})$$

$$A_{12} = -s\eta\ s2\eta_{td}$$

$$A_{13} = +c\eta\ s2\eta_{td}$$

$$A_{22} = -0.5\ (1 + c2\eta)\ (1 + c2\eta_{td}) + (1 - c2\eta_{td})$$

$$A_{23} = -0.5\ s2\eta\ (1 + c2\eta_{td})$$

$$A_{33} = +0.5\ (1 - c2\eta)\ (1 + c2\eta_{td}) - (1 - c2\eta_{td})$$

Appendix B gives a detailed derivation of equations (4) and (5) for the case where the x_{pr} axis is in the orbital plane, the z_{pr} axis has an elevation angle of η from the orbital plane and is generally pointing toward the sun (the z_v axis is pointing exactly toward the sun),[1] and the ϵ angles are small. The gravity gradient torque has been split into a nominal part $\underline{T}_{gn}$ which is not a function of the ϵ angles and a controllable part $\underline{T}_{gd}$, which will be used for the desaturation method. The nominal part shows that a bias momentum accumulates about the x_{pr} axis (Fig. 1); the others have only cyclic terms (Fig. 2). Visualization of $\underline{T}_{gn}$ as a function of time for an arbitrary moment-of-inertia distribution is described in Reference 7.

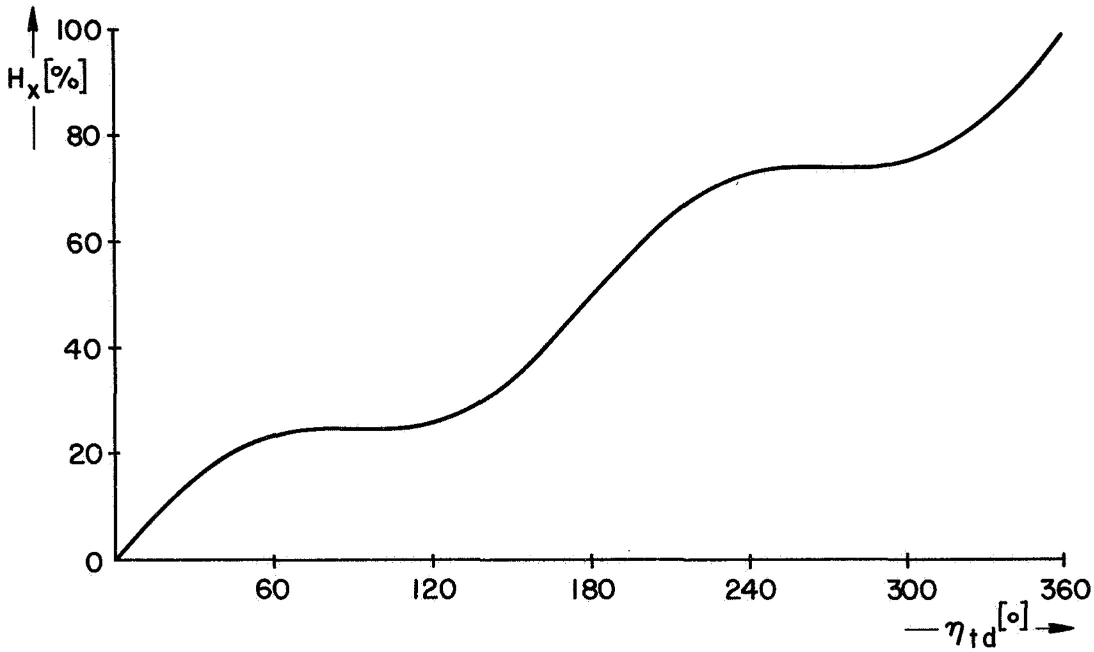

Figure 1. Angular momentum accumulation about the x_{pr} axis.

MOMENTUM DESATURATION METHOD

General

The development of a desaturation method using the gravity gradient torques consists of maneuvering the vehicle through angles (ϵ's) in such a way that the momentum accumulation caused by the angles desaturates the stored momentum to keep the total momentum bounded and to avoid the need for desaturation by the thruster attitude control system (TACS). The CMG attitude control system executes the ϵ angle commands.

---

1. η_{td} is the orbital angle from desaturation midnight (to be explained later).

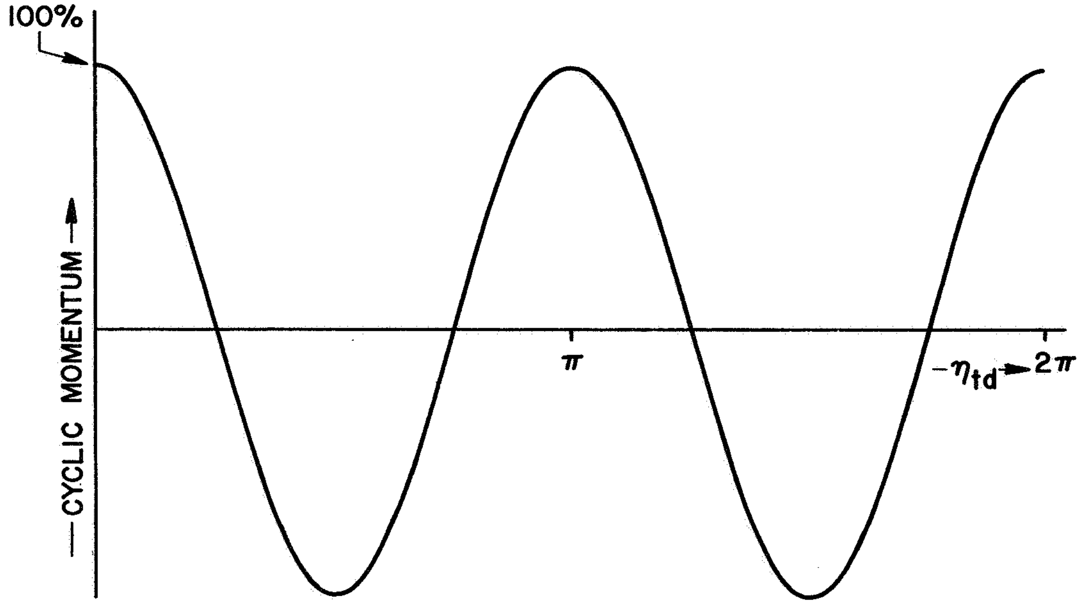

Figure 2. Typical cyclic angular momentum.

This system is described in References 2, 3, 4, and 5. The desaturation maneuvers must be consistent with the mission constraints which for Skylab allow maneuvers for part or all of the night portion of the orbit only. During the daylight part of the orbit, the ϵ angles must be zero except an angle about the vehicle z axis (sun line) which must be kept constant; therefore, the desaturation loop is only closed on a per orbit basis. The desaturation method can be separated into two parts. One part consists of the development of the desaturation momentum commands, using the total momentum profile. The other part consists of the generation of desaturation angles ϵ, given the desaturation momentum commands. The latter affects the former and is therefore presented first.

Desaturation Angle Generation

The angular momentum desaturated by a given set of ϵ angles is developed first. Since this momentum should be equal to the command, the equations are then inverted. Inspection of the A_{ij}'s reveals that they are either even or odd functions of η_{td}. Therefore, assuming that we have one set of constant angles before midnight, $\underline{\epsilon} + \underline{\Delta\epsilon}$, another set after midnight, $\underline{\epsilon} - \underline{\Delta\epsilon}$, and the integration interval is from $\eta_{td} = -\rho$ to $\eta_{td} = +\rho$, we get (Appendix C)

$$
\underline{H}_d = \begin{bmatrix} +a_{11} & 0 & 0 \\ 0 & +a_{22} & +a_{23} \\ 0 & -a_{23} & +a_{33} \end{bmatrix} \begin{bmatrix} \epsilon_x/A_1 \\ \epsilon_y/A_2 \\ \epsilon_z/A_3 \end{bmatrix}
+ \begin{bmatrix} 0 & +a_{12} & +a_{13} \\ -a_{12} & 0 & 0 \\ -a_{13} & 0 & 0 \end{bmatrix} \begin{bmatrix} \Delta\epsilon_x/A_1 \\ \Delta\epsilon_y/A_2 \\ \Delta\epsilon_z/A_3 \end{bmatrix} \tag{6}
$$

with

$$a_{11} = c2\eta\ (2\rho + s2\rho)$$

$$a_{12} = s\eta\ (1 - c2\rho)$$

$$a_{13} = -c\eta\ (1 - c2\rho)$$

$$a_{22} = -0.5\ (1 + c2\eta)\ (2\rho + s2\rho) + (2\rho - s2\rho)$$

$$a_{23} = -0.5\ s2\eta\ (2\rho + s2\rho)$$

$$a_{33} = 0.5\ (1 - c2\eta)\ (2\rho + s2\rho) - (2\rho - s2\rho)$$

$$A_1 = 2/(3\Omega\ \Delta I_x)$$

$$A_2 = 2/(3\Omega\ \Delta I_y)$$

$$A_3 = 2/(3\Omega\ \Delta I_z)$$

The moment-of-inertia distribution of the Skylab was configured so that ΔI_x is small, resulting in a small bias momentum accumulation. But a small ΔI_x makes the use of an ϵ_x or $\Delta\epsilon_x$ very ineffective for momentum desaturation, leading to the conclusion that no maneuvers about the x_p axis will be made, and we have as components of $\underline{H}_d$

$$H_{dx} = -a_{12}\,\Delta\epsilon_y/(-A_2) + a_{13}\,\Delta\epsilon_z/A_3 \tag{7}$$

$$\begin{bmatrix} H_{dy} \\ H_{dz} \end{bmatrix} = \begin{bmatrix} -a_{22} & a_{23} \\ a_{23} & a_{33} \end{bmatrix} \begin{bmatrix} \epsilon_y/(-A_2) \\ \epsilon_z/A_3 \end{bmatrix} \tag{8}$$

Equation (8) can be rewritten in the following form:

$$\begin{bmatrix} H_{dy} \\ H_{dz} \end{bmatrix} = \begin{bmatrix} c\eta & s\eta \\ -s\eta & c\eta \end{bmatrix} \begin{bmatrix} 2s2\rho & 0 \\ 0 & -(2\rho - s2\rho) \end{bmatrix} \begin{bmatrix} c\eta & -s\eta \\ s\eta & c\eta \end{bmatrix} \begin{bmatrix} \epsilon_y/(-A_2) \\ \epsilon_z/A_3 \end{bmatrix} \tag{9}$$

Equation (9) shows that resolution into the orbital plane decouples the equation.

It has been assumed so far that the ϵ angles can be reached instantaneously. In the following, the angle profiles of Figure 3 are substituted. The difference between the ideal and the actual momentum desaturated is expressed by an efficiency, and we have (the components are in the orbital coordinate system CS X_{pr})

$$\left(H_{dx}\right)_{act} = E_x\left(H_{dx}\right)_{id}$$

$$\left(H_{dy}\right)_{act} = E_y\left(H_{dy}\right)_{id}$$

$$\left(H_{dz}\right)_{act} = E_z\left(H_{dz}\right)_{id}$$

where

$$E_x = (2s\rho - s2\rho)/[\rho(1 - c2\rho)]$$

$$E_y = (c\rho - c2\rho)/(\rho\; s2\rho)$$

$$E_z = [3\rho/2 - (c\rho - c2\rho)/\rho]/(2\rho - s2\rho)$$

Appendix D gives a detailed development of the E's. Equations (7) and (9) become

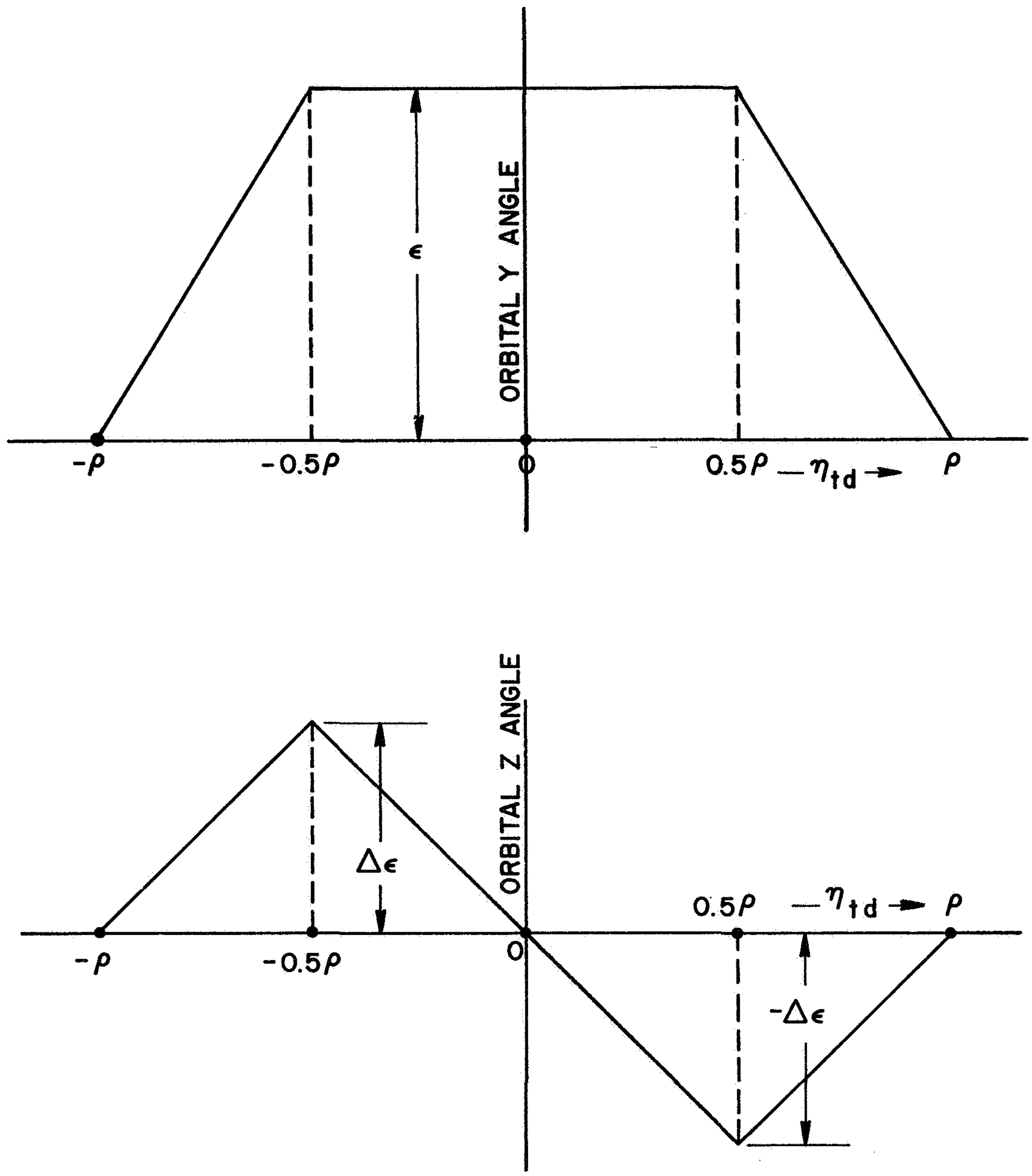

Figure 3. Desaturation angle profiles.

$$H_{dx} = -[(2s\rho - s2\rho)/\rho]\ [s\eta\ \Delta\epsilon_y/(-A_2) + c\eta\ \Delta\epsilon_z/A_3] \tag{10}$$

$$\begin{bmatrix} H_{dy} \\ H_{dz} \end{bmatrix} = \begin{bmatrix} c\eta & s\eta \\ -s\eta & c\eta \end{bmatrix} \begin{bmatrix} a_y & 0 \\ 0 & a_z \end{bmatrix} \begin{bmatrix} c\eta & -s\eta \\ s\eta & c\eta \end{bmatrix} \begin{bmatrix} \epsilon_y/(-A_2) \\ \epsilon_z/A_3 \end{bmatrix} \tag{11}$$

with

$$a_y = 2(c\rho - c2\rho)/\rho$$

$$a_z = -3\rho/2 + (c\rho - c2\rho)/\rho$$

Before inverting equations (10) and (11) it is necessary to discuss the orbital desaturation parameters a_y and a_z. The behavior of a_y for varying desaturation percentages (or varying ρ), normalized with respect to its maximum value, is shown as

$$F_1 = \frac{(c\rho - c2\rho)/\rho}{\text{MAX}\ [(c\rho - c2\rho)/\rho]}$$

in Figure 4. For a given orbital ϵ_y the maximum momentum is desaturated at a desaturation percentage of 32.1 percent ($\rho = 57.8°$). Instead of assuming a given angle we can assume that a constant maneuver momentum is available and that the maneuver angle is proportional to the available desaturation time. This is shown as

$$F_2 = \frac{c\rho - c2\rho}{\text{MAX}\ (c\rho - c2\rho)}$$

The peak of the orbital y-momentum desaturation shifts to a desaturation percentage of 42 percent ($\rho = 75.5°$), which is higher than the maximum nighttime available on Skylab (slightly less than 40 percent).

A comparison of the orbital z-momentum parameter a_z shows that even at the maximum desaturation percentage (about 40 percent) the same angle would only desaturate about one fourth in z as would in y. On the other hand, a constant angle about the

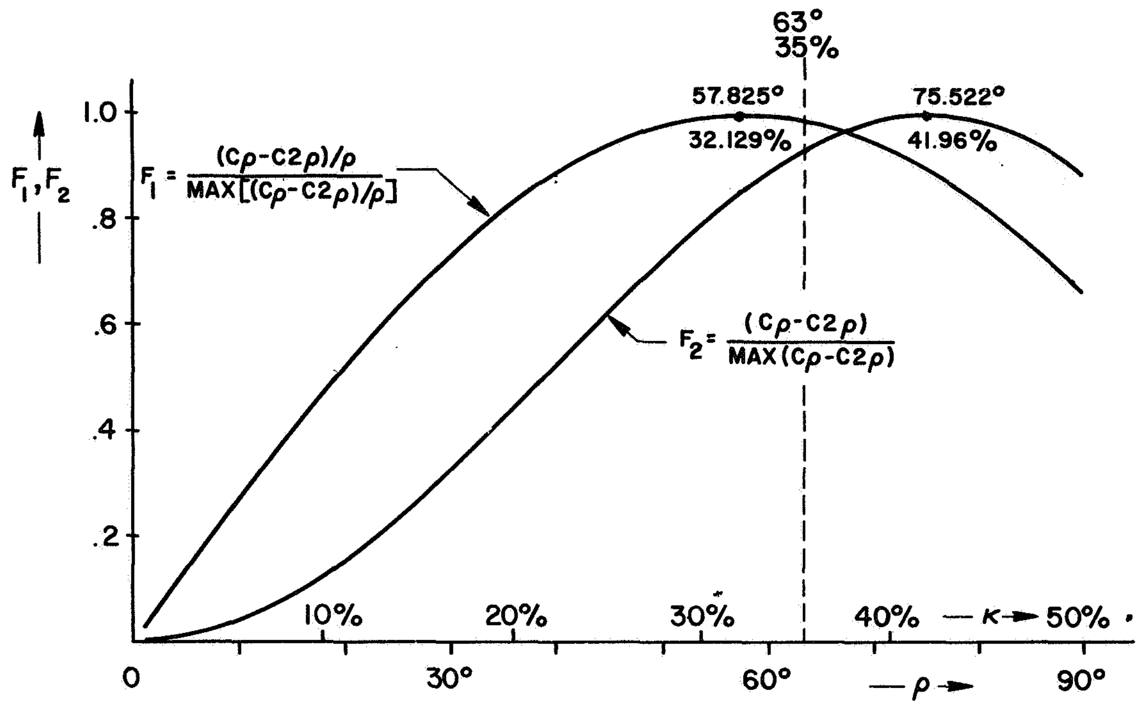

Figure 4. Relative desaturation capacity about orbital y axis.

z axis (if held for one orbit) is more than three times as effective as the same angle in y. Since mission constraints allow a constant angle about the vehicle z axis (which desaturates only orbital z momentum), it will be used exclusively for orbital z desaturation (the appropriate relationships are developed later).

Equations (10) and (11) show the actually desaturated momentum for a given set of desaturation angles and the maneuver profile of Figure 3. Assuming that the actual and the commanded momentum are equal, we can invert these equations. However, one more constraint must be added to equation (10). If we minimize $[\Delta\epsilon_y/(-A_2)]^2 + [\Delta\epsilon_z/A_3]^2$ (minimum maneuver momentum for $I_y = I_z$), inversion yields

$$\begin{bmatrix} \Delta\epsilon_y/(-A_2) \\ \Delta\epsilon_z/A_3 \end{bmatrix} \mp \frac{-\rho\, H_{dx}}{2s\rho - s2\rho} \begin{bmatrix} s\eta \\ c\eta \end{bmatrix} \tag{12}$$

Inversion of equation (11) results in

$$\begin{bmatrix} \epsilon_y/(-A_2) \\ \epsilon_z/A_3 \end{bmatrix} = \begin{bmatrix} c\eta & s\eta \\ -s\eta & c\eta \end{bmatrix} \begin{bmatrix} 1/a_y & 0 \\ 0 & 1/a_z \end{bmatrix} \begin{bmatrix} c\eta & -s\eta \\ s\eta & c\eta \end{bmatrix} \begin{bmatrix} H_{dy} \\ H_{dz} \end{bmatrix} \tag{13}$$

The assumption that all of the orbital z momentum, $H_{dzo} = s\eta H_{dy} + c\eta H_{dz}$, will be desaturated by a rotation about the vehicle z axis allows us to set $1/a_z$ to zero; thus

$$\begin{bmatrix} \epsilon_y/(-A_2) \\ \epsilon_z/A_3 \end{bmatrix} = [(c\eta H_{dy} - s\eta H_{dz})/a_y] \begin{bmatrix} c\eta \\ -s\eta \end{bmatrix} \tag{14}$$

The effectiveness (per orbit) of a rotation $\Delta\upsilon_z$ about the vehicle z axis must be calculated to justify this assumption. Evaluation of equation (9) for $\rho = \pi$ yields this effectiveness, where it is again assumed that $\Delta I_x'$ is negligibly small (no H_{dx}):

$$\begin{bmatrix} H_{dy} \\ H_{dz} \end{bmatrix}_{\Delta\upsilon_z} = \begin{bmatrix} c\eta & s\eta \\ -s\eta & c\eta \end{bmatrix} \begin{bmatrix} 0 & 0 \\ 0 & -2\pi \end{bmatrix} \begin{bmatrix} c\eta & -s\eta \\ s\eta & c\eta \end{bmatrix} \begin{bmatrix} 1/(-A_2) & 0 \\ 0 & 1/A_3 \end{bmatrix} \begin{bmatrix} K_{22} & K_{23} \\ K_{32} & K_{33} \end{bmatrix} \begin{bmatrix} 0 \\ \Delta\upsilon_z \end{bmatrix}$$

or

$$H_{dzo} = -2\pi\, [K_{23}\, s\eta/(-A_2) + K_{33}\, c\eta/A_3\,]\, \Delta\upsilon_z \tag{15}$$

where

$$[K] = \begin{bmatrix} K_{11} & K_{12} & K_{13} \\ K_{21} & K_{22} & K_{23} \\ K_{31} & K_{32} & K_{33} \end{bmatrix}$$

is the transformation matrix from vehicle axes to principal axes. Equation (15) shows that $\Delta\upsilon_z$ about the vehicle z axis is still only effective for orbital z-momentum desaturation, when considered on a per orbit basis, and does not couple into orbital y-momentum desaturation (which was to be shown). Some difficulties remain in the area of command generation which will be discussed later. Inversion of equation (15) results in

$$\Delta \upsilon_z = - H_{dzo} \Big/ \left\{ 2\pi [K_{23} s\eta/(-A_2) + K_{33} c\eta/A_2] \right\}$$

$$= - (s\eta H_{dy} + c\eta H_{dz}) \Big/ \left\{ 2\pi [K_{23} s\eta/(-A_2) + K_{33} c\eta/A_2] \right\}$$

The following approximation can be employed:

$$c\eta_x/A_4 = K_{23} s\eta/(-A_2) + K_{33} c\eta/A_3$$

which assumes that the moment-of-inertia misalignment is mostly about the x axis ($K_{11} \approx 1$) and that $I_y \approx I_z$ such that an average can be used.

$$A_4 = 0.5[(-A_2) + A_3] \tag{17}$$

In summary, given three momentum components H_{dx}, H_{dy}, and H_{dz} in principal coordinates, the desaturation angle commands in vehicle coordinates are

$$\Delta \upsilon_z = -A_4 (s\eta H_{dy} + c\eta H_{dz})/(2\pi c\eta_x) \tag{18}$$

$$\begin{bmatrix} \Delta\epsilon_x \\ \Delta\epsilon_y \\ \Delta\epsilon_z \end{bmatrix} = \begin{bmatrix} K_{11} & K_{21} & K_{31} \\ K_{12} & K_{22} & K_{32} \\ K_{13} & K_{23} & K_{33} \end{bmatrix} \begin{bmatrix} 0 \\ s\eta(-A_2) \\ c\eta A_3 \end{bmatrix} [-\rho/(2s\rho - s2\rho)] H_{dx} \tag{19}$$

$$\begin{bmatrix} \epsilon_x \\ \epsilon_y \\ \epsilon_z \end{bmatrix} = \begin{bmatrix} K_{11} & K_{21} & K_{31} \\ K_{12} & K_{22} & K_{32} \\ K_{13} & K_{23} & K_{33} \end{bmatrix} \begin{bmatrix} 0 \\ c\eta(-A_2) \\ -s\eta A_3 \end{bmatrix} \frac{\rho(c\eta H_{dy} - s\eta H_{dz})}{2(c\rho - c2\rho)} \tag{20}$$

Equations (19) and (20) assume that the desaturation angle commands are applied according to the profiles in Figure 3 and equation (18) assumes that $\Delta \upsilon_z$ is applied for a full orbit (where the change in υ_z is made right after the desaturation interval at $\eta_{td} = +\rho$; see Appendix E for nominal υ_z angle).

The maneuver commands before midnight are then (these angles are reached at $\eta_{td} = -\rho/2$)

$$\begin{bmatrix} \epsilon_{x1} \\ \epsilon_{y1} \\ \epsilon_{z1} \end{bmatrix} = \begin{bmatrix} \epsilon_x \\ \epsilon_y \\ \epsilon_z \end{bmatrix} + \begin{bmatrix} \Delta\epsilon_x \\ \Delta\epsilon_y \\ \Delta\epsilon_z \end{bmatrix} \tag{21}$$

The commands after midnight are (these angles are reached at $\eta_{td} = \rho/2$)

$$\begin{bmatrix} \epsilon_{x2} \\ \epsilon_{y2} \\ \epsilon_{z2} \end{bmatrix} = \begin{bmatrix} \epsilon_x \\ \epsilon_y \\ \epsilon_z \end{bmatrix} - \begin{bmatrix} \Delta\epsilon_x \\ \Delta\epsilon_y \\ \Delta\epsilon_z \end{bmatrix} \tag{22}$$

The maneuver commands of equations (21) and (22) disregard the fact that the CMG's may not have sufficient momentum reserve available to execute the maneuver which will require reduction of the maneuver angle commands. This is treated in Appendix F.

Figure 5 shows a typical CMG momentum profile.

Angular Momentum Sampling

An adequate representation of the momentum accumulation of the Skylab is

$$\begin{aligned} \underline{H}_t = {} & \underline{H}_s \, s2(\eta_{td} - \pi) + \underline{H}_c \, c2(\eta_{td} - \pi) \\ & + \underline{H}_k(\eta_{td} - \pi)/(2\pi) + (\underline{H}_a + \underline{H}_b) \end{aligned} \tag{23}$$

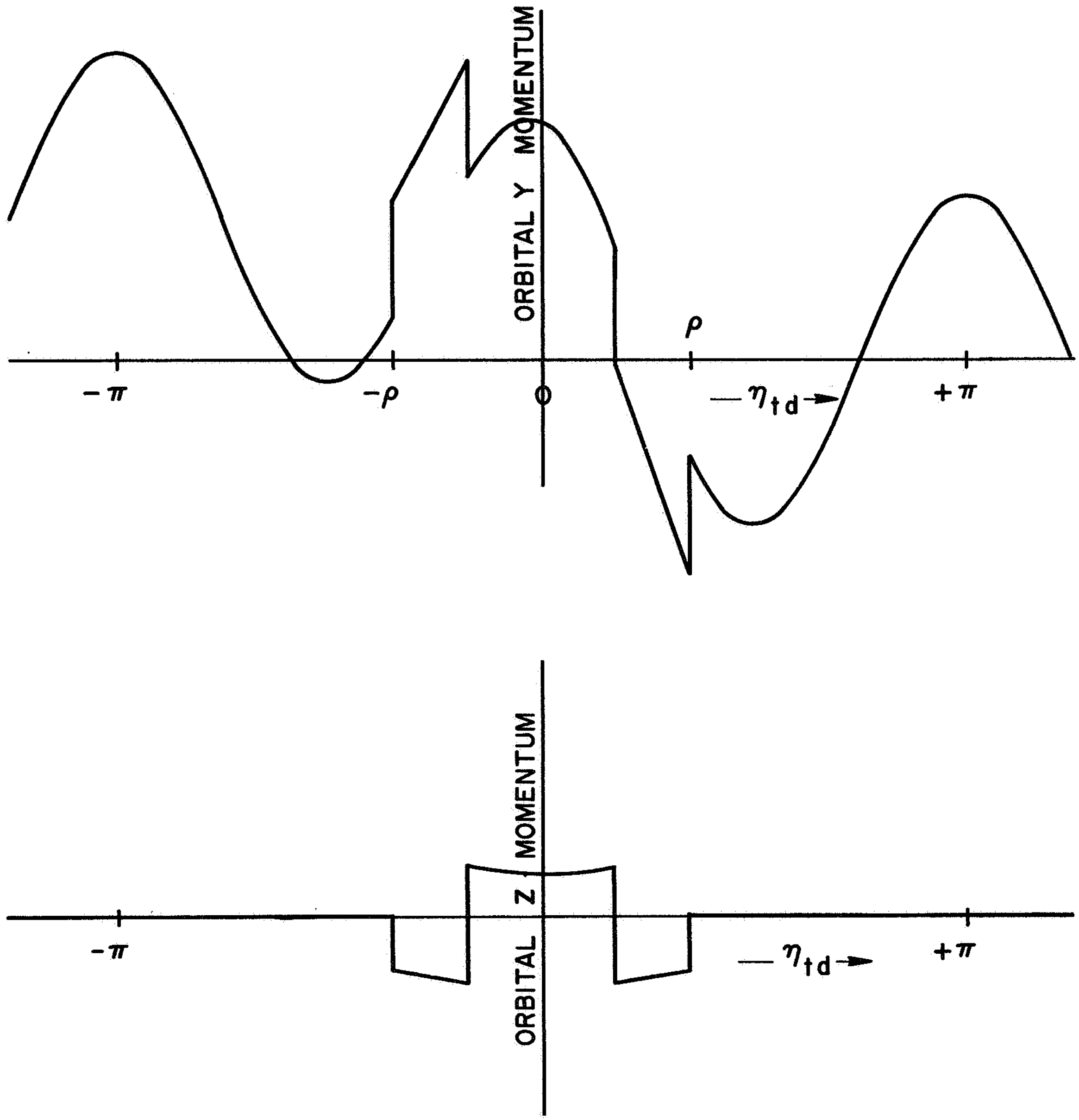

Figure 5. Typical CMG momentum profile.

where $\eta_{td} = \Omega t$, $\underline{H}_s$ and $\underline{H}_c$ are the amplitudes of the cyclic components (see Appendix G), $\underline{H}_k$ is the momentum per orbit caused by a constant torque or constant angle, and $\underline{H}_a$ is the average momentum at noon in excess of the desired bias $\underline{H}_b$ [equation (23) is set up with respect to noon and η_{td} is with respect to midnight].

The task of the desaturation method is to center the cyclic components about some given bias point ($\underline{H}_b$), which is normally zero. This necessitates a determination of $\underline{H}_a$ and $\underline{H}_k$. To accomplish this, the total system momentum is sampled at four points in orbit as shown in Figure 6. The total system momentum is used rather than the CMG momentum only to avoid invalid readings in case the vehicle is maneuvering at the time the sample is taken. The sample points are at $2(\pi/4)$, $3(\pi/4)$, $5(\pi/4)$, and $6(\pi/4)$ and accordingly carry the subscripts 2, 3, 5, and 6.

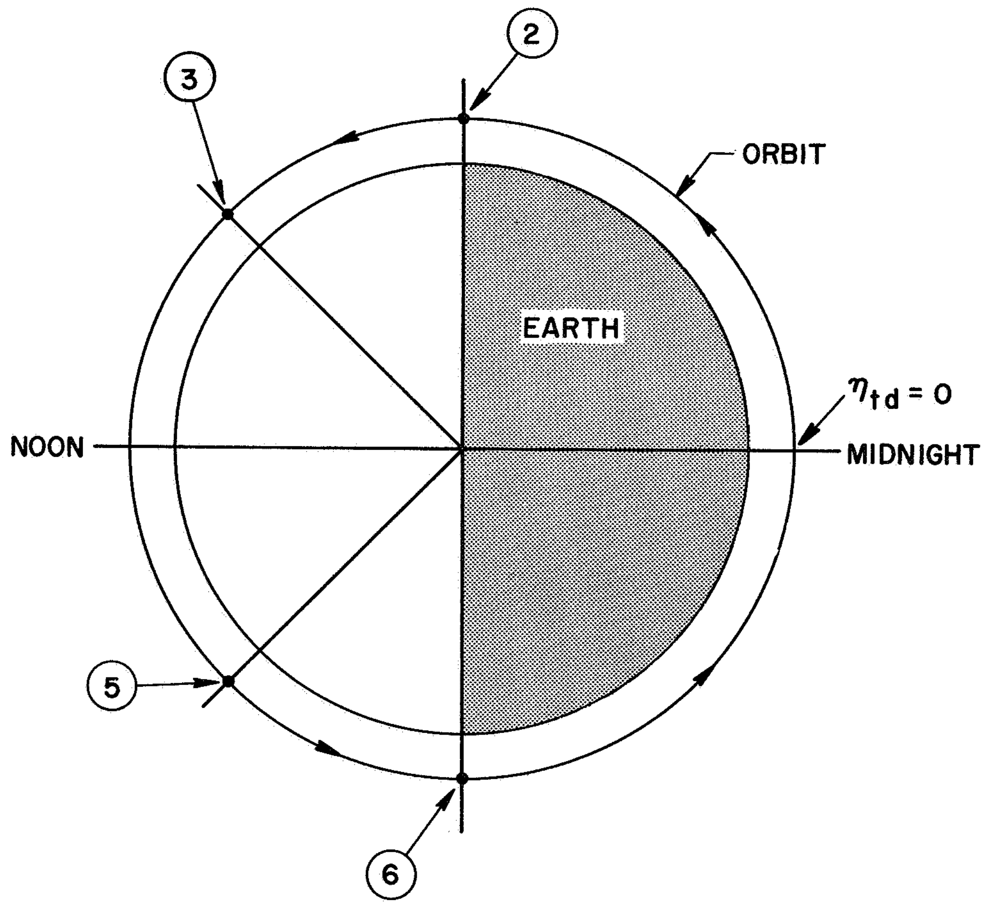

Figure 6. Orbital angular momentum sampling points.

Evaluation of equation (23) at the sample points results in

$$\begin{bmatrix} \underline{H}_{t2} \\ \underline{H}_{t3} \\ \underline{H}_{t5} \\ \underline{H}_{t6} \end{bmatrix} = \begin{bmatrix} 0 & -1 & -0.25 & +1 \\ -1 & 0 & -0.25 & +1 \\ +1 & 0 & +0.25 & +1 \\ 0 & -1 & +0.25 & +1 \end{bmatrix} \begin{bmatrix} \underline{H}_s \\ \underline{H}_c \\ \underline{H}_k \\ \underline{H}_a + \underline{H}_b \end{bmatrix} \tag{24}$$

Inversion of equation (24) yields

$$\begin{bmatrix} \underline{H}_s \\ \underline{H}_c \\ \underline{H}_k \\ \underline{H}_a + \underline{H}_b \end{bmatrix} = \begin{bmatrix} +0.25 & -0.5 & +0.5 & -0.25 \\ -0.5 & +0.5 & +0.5 & -0.5 \\ -2 & 0 & 0 & +2 \\ 0 & +0.5 & +0.5 & 0 \end{bmatrix} \begin{bmatrix} \underline{H}_{t2} \\ \underline{H}_{t3} \\ \underline{H}_{t5} \\ \underline{H}_{t6} \end{bmatrix} \tag{25}$$

It should be recognized that as far as $\underline{H}_k$ and $(\underline{H}_a + \underline{H}_b)$ are concerned, only the spacing of the sample points is important; their relationship to η_{td} is immaterial.

Desaturation Command Generation

A desaturation command of the form

$$\underline{H}_d = -\underline{H}_a \tag{26}$$

would result (in steady state) in an offset of $\underline{H}_a = \underline{H}_k$ since $\underline{H}_k$ must be desaturated each orbit. The following form would eliminate (for the ideal case) the offset:

$$\underline{H}_d = -(\underline{H}_a + \underline{H}_k) \tag{27}$$

The nonideal case (tolerances in the momentum measurements, etc.) still results in an offset.

A form that eliminates steady state offsets is

$$\underline{H}_d = \Sigma \underline{H}_a - \underline{H}_k \tag{28}$$

with

$$\Sigma \underline{H}_a = \Sigma \underline{H}_{a(n-1)} - \underline{H}_a + 0.75\ \underline{H}_{a(n-1)} \tag{29}$$

where (n-1) indicates the value for the past orbit. Any steady state signal needed will now be provided by $\Sigma \underline{H}_a$, a computed quantity, rather than by a physical offset ($\underline{H}_a$). The sampled data characteristics of equations (28) and (29) are treated in Appendix H.

The fact that a υ_z-angle is utilized for desaturation of the orbital angular momentum component introduces a difficulty: A ıamp in the orbital z momentum must be considered as having been introduced by the desaturation itself and its effect on $\underline{H}_{az}$ must be compensated. A simple example will illustrate the point. Consider only an initial momentum about the orbital z axis. This momentum is measured as $(H_{az})_1 = H_o$ during the first orbit. At the end of the first desaturation interval, υ_z is changed by $\Delta\upsilon_z$ so that H_o is eliminated after exactly one orbit. But at noon of the second orbit, υ_z has not done its job yet, and $(H_{az})_2$ measures the remaining momentum (about 0.55 H_o for a 35 percent desaturation). This remaining momentum is

$$(H_{rz})_2 = -0.55\ (H_{kz})_2 \qquad \left[\text{since } (H_{kz})_2 = -(H_{az})_1\right]$$

and it must be subtracted from the orbital z momentum:

$$(H_{az})_2 = \frac{1}{2}\ (H_{tz3} + H_{tz5})_2 + 0.555\ (H_{kz})_2 \tag{30}$$

For the example $(H_{az})_2$ would be zero and $(H_{kz})_2$ would have the right value to eliminate exactly the previously introduced $\Delta\upsilon_z$. Equation (30) seemingly contradicts the comments made with respect to equation (26), but it should be recognized that in steady state there is no H_{koz}; i.e., whatever average torques are acting about orbital z are compensated for by the appropriate υ_z.

In a sense, the latter fact is a gravity gradient sensor holding the vehicle in a certain attitude about the sun line. It holds this attitude also if there is rate gyro drift, which is compensated for on a per orbit basis by the appropriate $\Delta \upsilon_z$. Since the external torques (besides gravity gradient) are unknown, it is impossible to state what attitude is maintained. For attitude control, a combination rate gyro/strapdown reference calculation is sufficient, but a star tracker or other reference is necessary for exact knowledge of the attitude about the sun line.

The desaturation momentum commands used in equations (18), (19), and (20) are in principal coordinates, but the angular momentum samples and the desired momentum bias are in vehicle coordinates. Therefore,

$$\underline{H}_k = 2[K] \, (\underline{H}_{t6} - \underline{H}_{t2}) \tag{31}$$

$$\underline{H}_a = [K] \left[0.5 \, (\underline{H}_{t3} + \underline{H}_{t5}) - \underline{H}_b\right] + 0.555 \, [\eta] \, [0,0,(s\eta H_{ky} + c\eta H_{kz})]^T \tag{32}$$

$$\Sigma \underline{H}_a = \Sigma \underline{H}_a - \underline{H}_a + 0.75 \, \underline{H}_{a(n-1)} \tag{33}$$

$$\underline{H}_d = \Sigma \underline{H}_a - \underline{H}_k \tag{34}$$

So far it has not been considered that the CMG's can saturate, but if they do, a minimum impulse bit (MIB) must be fired in the appropriate direction by the TACS to desaturate the CMG's immediately or fine pointing is lost. Therefore, the momentum desaturated by the MIB's must be included in the samples, or $\underline{H}_a$ and $\underline{H}_k$ give erroneous results:

$$\underline{H}_{ti} = \underline{H}_t - \Sigma \underline{H}_{mib} \quad (i = 2, 3, 5, 6)$$

where $\underline{H}_t$ is the total system momentum at the sample time and $\Sigma \underline{H}_{mib}$ is the accumulated MIB momentum fromthe time of the first sample $(i = 2)$ to the time of the present sample. $\underline{H}_k$ can then be calculated as usual [equation (25)], but $\underline{H}_a$ becomes

$$\underline{H}_a = 0.5 \, (\underline{H}_{t3} + \underline{H}_{t5}) - \underline{H}_b + \Sigma \underline{H}_{mib} \tag{35}$$

where $\Sigma \underline{H}_{mib}$ is the accumulated MIB momentum from the first sample until the time of execution of equation (35); thus whatever momentum the MIB's have already desaturated does not need to be desaturated by maneuvers.

APPENDIX A

DEFINITIONS OF SKYLAB COORDINATE SYSTEMS AND ANGLES

Only the coordinate systems (CS's) needed for the development of the desaturation method are defined. Some transformations are shown for completeness, but are not needed for the development, which is pointed out in the definitions (e.g., for X_r: η_y-angle is not needed). All CS's are right handed and orthogonal. All angles are defined mathematically positive and those with a t subscript are orbital y angles.

Symbols	Transformation Matrix	Definition
x_o, y_o, z_o	N/A	Basic orbital CS. z_o toward ascending node; y_o toward orbital north. (CS X_o is not needed explicitly for desaturation method.)
x_r, y_r, z_r	$X_r = [\eta_x]\ [\eta_y]\ X_o$	Reference CS. z_r toward sun; x_r in the orbital plane; y_r in northern orbital hemisphere. (η_y angle is not needed.)
x_{or}, y_{or}, z_{or}	$X_{or} = [\eta_x]^T\ X_r$	Orbital reference CS. z_{or} along projection of z_r into orbital plane; y_{or} toward orbital north.
x_d, y_d, z_d	$X_d = [\eta_t]\ X_{or}$	Disturbance CS. z_d toward center of earth; y_d toward orbital north. ($\eta_t = 0$ indicates orbital midnight; η_t is a y angle.)
x_{vr}, y_{vr}, z_{vr}	$X_{vr} = [\upsilon_z]\ X_r$	Vehicle reference CS. For no attitude deviation the vehicle geometric axes will be aligned with this CS.

Symbol	Transformation Matrix	Definition
x_v y_v z_v	$X_v = [\phi_e]\ X_{vr}$	Vehicle geometric CS. z_v toward the ATM rack; x_v toward CSM. $[\phi_e]$ is the attitude deviation (commanded or error.)
x_p y_p z_p	$X_p = [K]\ X_v$	Principal axis CS. Axes along principal moment-of-inertia axes; labeling of the axes such that tr[K] is maximized.
x_{pr} y_{pr} z_{pr}	$X_{pr} = [K]\ X_{vr}$	Principal axes reference CS. This is the CS for the principal axes in the absence of an attitude deviation.
x_{op} y_{op} z_{op}	$X_{op} = [\upsilon_{zp}]^T\ [\eta]^T\ X_{pr}$	Orbital principal CS. z_{op} along the projection of z_{pr} into the orbital plane; y_{op} toward orbital north. (υ_{zp} is not needed.)
x_{pr} y_{pr} z_{pr}	$X_{pr} = [\eta_{xp}]\ [\upsilon_{ze}]\ [\eta_{tm}]\ X_{or}$	Another definition of the CS X_{pr} showing the angles η_{tm} and υ_{ze} which are used in Appendix G. (η_{xp} is not needed.)

APPENDIX B

DERIVATION OF GRAVITY GRADIENT TORQUE

The gravity gradient torque acting on the vehicle is [equation (2)]

$$\underline{T}_g = 3\Omega^2 [\tilde{r}_{pr}] [\epsilon]^T [I_p] [\epsilon] \underline{r}_{pr} \tag{B1}$$

with

$$[I_p] = \begin{bmatrix} I_x & 0 & 0 \\ 0 & I_y & 0 \\ 0 & 0 & I_z \end{bmatrix}$$ principal moment-of-inertia matrix

where

Ω orbital rate for circular orbit

$\underline{r}_{pr}$ unit vector parallel to radius vector from the center of the earth to the vehicle center of mass

$[\epsilon]$ transformation matrix from the principal reference CS X_{pr} to the principal axes CS X_p

In the following development it is assumed that the ϵ angles are small and that x_{pr} lies in the orbital plane and z_{pr} points toward the center of the sun. Equation (2) can be written as

$$\underline{T}_g = 3\Omega^2 [\tilde{r}_{pr}] \left\{ [E] + [\tilde{\epsilon}] \right\} [I_p] \left\{ [E] - [\tilde{\epsilon}] \right\} \underline{r}_{pr} \tag{B2}$$

with

$$[\tilde{\epsilon}] = \begin{bmatrix} 0 & -\epsilon_z & +\epsilon_y \\ +\epsilon_z & 0 & -\epsilon_x \\ -\epsilon_y & +\epsilon_x & 0 \end{bmatrix} \tag{B3}$$

where ϵ_x, ϵ_y, and ϵ_z are small angles about the corresponding principal axes and $[E]$ is the identity matrix.

The moment-of-inertia differences will appear so frequently in the following that new symbols are introduced:

$$\Delta I_x = I_z - I_y$$

$$\Delta I_y = I_x - I_z$$

$$\Delta I_z = I_y - I_x$$

Operating on equation (B2) leads to

$$\underline{T}_g = 3\Omega^2 [\tilde{r}_{pr}] \left\{ [I_p] - [I_p][\tilde{\epsilon}] + [\tilde{\epsilon}][I_p] - [\tilde{\epsilon}][I_p][\tilde{\epsilon}] \right\} \underline{r}_{pr}$$

The term $[\tilde{\epsilon}][I_p][\tilde{\epsilon}]$ contains only square terms in ϵ and is neglected.

$$T_g = 3\Omega^2 \begin{bmatrix} 0 & -r_z & +r_y \\ +r_z & 0 & -r_x \\ -r_y & +r_x & 0 \end{bmatrix} \begin{bmatrix} +I_x & -\Delta I_z \epsilon_y & -\Delta I_y \epsilon_y \\ -\Delta I_z \epsilon_z & +I_y & -\Delta I_x \epsilon_x \\ -\Delta I_y \epsilon_y & -\Delta I_x \epsilon_x & +I_z \end{bmatrix} \begin{bmatrix} r_x \\ r_y \\ r_z \end{bmatrix}$$

where r_x, r_y, and r_z are the components of $\underline{r}_{pr}$ in the principal reference CS X_{pr}

$$\underline{T} = 3\Omega^2 \left\{ \begin{bmatrix} \Delta I_x r_y r_z \\ \Delta I_y r_z r_x \\ \Delta I_z r_x r_y \end{bmatrix} + \begin{bmatrix} -r_y^2+r_z^2 & -r_x r_y & +r_x r_z \\ +r_y r_x & -r_z^2+r_x^2 & -r_y r_z \\ -r_z r_x & +r_z r_y & -r_x^2+r_y^2 \end{bmatrix} \begin{bmatrix} \Delta I_x \epsilon_x \\ \Delta I_y \epsilon_y \\ \Delta I_z \epsilon_z \end{bmatrix} \right\}$$

The torque has been split into two parts: one that is independent of the ϵ angles and can be considered the nominal part, and one that is dependent on the ϵ angles and can be controlled.

The components of $\underline{r}_{pr}$ are developed as follows:

$$\underline{r}_{pr} = [\eta] \, [\eta_{tm}] \, [\eta_t]^T \underline{r}_d = [\eta] \, [\eta_{td}]^T \underline{r}_d$$

with

$$[\eta_{td}] = [\eta_t - \eta_{tm}]$$

or

$$\begin{bmatrix} r_x \\ r_y \\ r_z \end{bmatrix} = \begin{bmatrix} 1 & 0 & 0 \\ 0 & c\eta & s\eta \\ 0 & -s\eta & c\eta \end{bmatrix} \begin{bmatrix} c\eta_{td} & 0 & s\eta_{td} \\ 0 & 1 & 0 \\ -s\eta_{td} & 0 & c\eta_{td} \end{bmatrix} \begin{bmatrix} 0 \\ 0 \\ -1 \end{bmatrix}$$

$$= - \begin{bmatrix} s\eta_{td} \\ s\eta \; c\eta_{td} \\ c\eta \; c\eta_{td} \end{bmatrix}$$

Consequently,

$$\underline{T}_g = \underline{T}_{gn} + \underline{T}_{gd}$$

with

$$\underline{T}_{gn} = 3\Omega^2 \begin{bmatrix} \Delta I_x \, s\eta \; c\eta \; c^2\eta_{td} \\ \Delta I_y \, c\eta \; s\eta_{td} \; c\eta_{td} \\ \Delta I_z \, s\eta \; s\eta_{td} \; c\eta_{td} \end{bmatrix}$$

$$\underline{T}_{gd} = \frac{3}{2}\Omega^2 \begin{bmatrix} +A_{11} & +A_{12} & +A_{13} \\ -A_{12} & +A_{22} & +A_{23} \\ -A_{13} & -A_{23} & +A_{33} \end{bmatrix} \begin{bmatrix} \Delta I_x \, \epsilon_x \\ \Delta I_y \, \epsilon_y \\ \Delta I_z \, \epsilon_z \end{bmatrix}$$

where

$$A_{11} = +2(c^2\eta - s^2\eta)\, c^2\eta_{td} = + c2\eta \,(1 + c2\eta_{td})$$

$$A_{12} = -2\, s\eta \; s\eta_{td} \; c\eta_{td} = - s\eta \; s2\eta_{td}$$

$$A_{13} = +2\, c\eta \; s\eta_{td} \; c\eta_{td} = + c\eta \; s2\eta_{td}$$

$$A_{22} = +2(s^2\eta_{td} - c^2\eta \; c^2\eta_{td}) = +(1 - c2\eta_{td}) - \frac{1}{2}(1 + c2\eta)(1 + c2\eta t_d)$$

$$A_{23} = -2\, s\eta \; c\eta \; c^2\eta_{td} = - \frac{1}{2} s2\eta \,(1 + c2\eta_{td})$$

$$A_{33} = -2(s^2\eta_{td} - s^2\eta \; c^2\eta_{td}) = + \frac{1}{2}(1 - c2\eta)(1 + c2\eta_{td}) - (1 - c2\eta_{td})$$

APPENDIX C

COEFFICIENT EVALUATION

The following definite integrals are involved in the development of the a_{ij} coefficients of equation (7) or (8)

$$\int_{-\rho}^{0} s2\eta_{td}\, d\eta_{td} = -\int_{0}^{\rho} s2\eta_{td}\, d\eta_{td} = -\frac{1}{2}(1 - c2\rho)$$

$$\int_{-\rho}^{0} (1 \pm c2\eta_{td})\, d\eta_{td} = \int_{0}^{\rho} (1 \pm c2\eta_{td})\, d\eta_{td} = +\frac{1}{2}(2\rho \pm s2\rho)$$

With these integrals, we obtain ($1/2\Omega$ has been absorbed in the A_i's)

$$a_{12} = 2\int_{-\rho}^{0} A_{12}\, d\eta_{td} = -2s\eta \int_{-\rho}^{0} s2\eta_{td}\, d\eta_{td} = +s\eta\,(1 - c2\rho)$$

$$a_{13} = 2\int_{-\rho}^{0} A_{13}\, d\eta_{td} = +2c\eta \int_{-\rho}^{0} s2\eta_{td}\, d\eta_{td} = -c\eta\,(1 - c2\rho)$$

$$a_{23} = 2\int_{-\rho}^{0} A_{23}\, d\eta_{td} = -s2\eta \int_{-\rho}^{0} (1 + c2\eta_{td})\, d\eta_{td} = -\frac{1}{2} s2\eta\,(2\rho + s2\rho)$$

$$a_{22} = 2\int_{-\rho}^{0} A_{22}\, d\eta_{td} = -(1 + c2\eta)\int_{-\rho}^{0} (1 + c2\eta_{td})\, d\eta_{td} + 2\int_{-\rho}^{0} (1 - c2\eta_{td})\, d\eta_{td}$$

$$= -\frac{1}{2}(1 + c2\eta)(2\rho + s2\rho) + (2\rho - s2\rho)$$

$$a_{33} = 2\int_{-\rho}^{0} A_{33}\, d\eta_{td} = +(1 + c2\eta)\int_{-\rho}^{0} (1 + c2\eta_{td})\, d\eta_{td} - \int_{-\rho}^{0} (1 - c2\eta_{td})\, d\eta_{td}$$

$$= +\frac{1}{2}\,(1 - c2\eta)\,(2\rho + s2\rho) - (2\rho - s2\rho)$$

APPENDIX D

DESATURATION MANEUVER EFFICIENCIES

The maneuver angles cannot be reached instantaneously because of the limited vehicle angular velocity imposed by CMG momentum limitations. The angle profiles of Figure 3 are therefore used and the ratios between the desaturated momentum by the actual angle profile and the one desaturated by the ideal profile are expressed as efficiencies:

$$E_x = \left(H_{dx}\right)_{act} / \left(H_{dx}\right)_{id}$$

$$E_y = \left(H_{dy}\right)_{act} / \left(H_{dy}\right)_{id}$$

$$E_z = \left(H_{dz}\right)_{act} / \left(H_{dz}\right)_{id}$$

where the components are in CS X_{pr}. The actual desaturated momentum can be interpreted as the integration over infinitely small maneuvers with 100 percent efficiency, but with varying desaturation percentage.

The ideal x desaturation momentum is

$$\left(H_{dx}\right)_{id} = (1 - c2\rho)\, \Delta\epsilon'$$

with

$$\Delta\epsilon' = s\eta\Delta\epsilon_y/(-A_2) - c\eta\Delta\epsilon_z/A_3$$

[cf. equation (7)]. The actual x desaturation momentum is

$$\left(H_{dx}\right)_{act} = \int_0^{\Delta\epsilon'} [1 - c2(\rho - \rho')]\, d\alpha - \int_0^{\Delta\epsilon'} [1 - c2\rho']\, d\alpha$$

where α is a dummy integration variable and

$$\rho' = \alpha\rho/(2\Delta\epsilon')$$

Evaluation leads to

$$\left(H_{dx}\right)_{act} = \int_0^{\Delta\epsilon'} \left[- c2\rho \left(1 - \frac{\alpha}{2\Delta\epsilon'}\right) + c\ \frac{\rho\alpha}{\Delta\epsilon'}\right] d\alpha$$

$$= \frac{\Delta\epsilon'}{\rho} \left[s2\rho \left(1 - \frac{\alpha}{2\Delta\epsilon'}\right) + s\ \frac{\rho\alpha}{\Delta\epsilon'}\right]_0^{\Delta\epsilon'}$$

$$= \frac{\Delta\epsilon'}{\rho} (2s\rho - s2\rho)$$

and

$$E_x = \frac{2s\rho - s2\rho}{\rho(a - c2\rho)} \tag{D1}$$

The ideal y desaturation momentum is

$$\left(H_{dy}\right)_{id} = 2s2\rho\ \epsilon_y'$$

with

$$\epsilon_y' = c\eta\epsilon_y/(-A_2) - s\eta\epsilon_z/A_3$$

[see equation (9)]. The actual y desaturation momentum is

$$\left(H_{dy}\right)_{act} = 2 \int_0^{\epsilon_y'} s2(\rho - \rho')\, d\alpha$$

with

$$\rho' = \alpha\rho/(2\epsilon_y')$$

Evaluation leads to

$$\left(H_{dy}\right)_{act} = 2 \int_0^{\epsilon_y'} s2\rho \left(1 - \frac{\alpha}{2\epsilon_y'}\right) d\alpha$$

$$= \frac{2\epsilon_y'}{\rho}\, c2\rho \left(1 - \frac{\alpha}{2\epsilon_y'}\right) \Big|_0^{\epsilon_y'}$$

$$= \frac{2\epsilon_y'}{\rho} (c\rho - c2\rho)$$

and

$$E_y = \frac{c\rho - c2\rho}{\rho\, s2\rho} \tag{D2}$$

Note that E_y is always larger than one (for the desaturation percentages considered) since the actual angle profile has less losses at the beginning and the end of the desaturation interval than the ideal profile (the torques are a function of $c2\eta_{td}$).

The ideal z desaturation momentum is

$$\left(H_{dz}\right)_{id} = -(2\rho - s2\rho)\, \epsilon_z'$$

with

$$\epsilon_z' = s\eta\epsilon_y/(-A_2) + c\eta\epsilon_z/A_3$$

[see equation (9)]. The actual z desaturation momentum is

$$(H_{dz})_{act} = - \int_0^{\epsilon_z'} [2(\rho - \rho') - s2(\rho - \rho')] \, d\alpha$$

where

$$\rho' = \alpha\rho/(2\epsilon_z')$$

Evaluation yields

$$\left(H_{dz}\right)_{act} = - \int_0^{\epsilon_z'} \left[2\rho\left(1 - \frac{\alpha}{2\epsilon_z'}\right) - s2\rho\left(1 - \frac{\alpha}{2\epsilon_z'}\right)\right] d\alpha$$

$$= - 2\rho \left[\alpha - \frac{\alpha^2}{4\epsilon_z'}\right]_0^{\epsilon_z'} + \frac{\epsilon_z'}{\rho} \, c2\rho \left[1 - \frac{\alpha}{2\epsilon_z'}\right]_0^{\epsilon_z'}$$

$$= - \left[\frac{3}{2}\rho - \frac{1}{\rho}(c\rho - c2\rho)\right]\epsilon_z'$$

and

$$E_z = \frac{\frac{3}{2}\rho - \frac{1}{\rho}(c\rho - c2\rho)}{2\rho - s2\rho} \qquad \text{(D3)}$$

APPENDIX E

ORBITAL ELEVATION OF PRINCIPAL z_p AXIS, NOMINAL ROTATION υ_{zg} ABOUT THE SUN LINE, AND GRAVITY GRADIENT TORQUE PHASE SHIFT η_{tm}

The sine and cosine functions of the orbital elevation η of the principal z_p axis are needed for equations (18), (19), and (20) and must be calculated from the known vehicle angles η_x and υ_z and the principal axes misalignment $[K]$. The transformation from orbital reference coordinates to principal reference coordinates is

$$[c] = [K]\ [\upsilon_z]\ [\eta_x] \tag{E1}$$

which results in

$$c_{11} = K_{11}\, c\upsilon_z - K_{12}\, s\upsilon_z$$

$$c_{12} = (K_{11}\, s\upsilon_z + K_{12}\, c\upsilon_z)c\eta_x - K_{13}\, s\eta_x$$

$$c_{13} = (K_{11}\, s\upsilon_z + K_{12}\, c\upsilon_z)s\eta_x + K_{13}\, c\eta_x$$

$$c_{21} = K_{21}\, c\upsilon_z - K_{22}\, s\upsilon_z$$

$$c_{22} = (K_{21}\, s\upsilon_z + K_{22}\, c\upsilon_z)c\eta_x - K_{23}\, s\eta_x$$

$$c_{23} = (K_{21}\, s\upsilon_z + K_{22}\, c\upsilon_z)s\eta_x + K_{23}\, c\eta_x$$

$$c_{31} = K_{31}\, c\upsilon_z - K_{32}\, s\upsilon_z$$

$$c_{32} = (K_{31}\, s\upsilon_z + K_{32}\, c\upsilon_z)c\eta_x - K_{33}\, s\eta_x$$

$$c_{33} = (K_{31}\, s\upsilon_z + K_{32}\, c\upsilon_z)s\eta_x + K_{33}\, c\eta_x$$

For the sine function of the elevation η of the principal z_p axis we have (the attitude error is assumed zero)

$$s\eta = -c_{32} = K_{33}\,s\eta_x - (K_{31}\,s\upsilon_z + K_{32}\,c\upsilon_z)s\eta_x \tag{E2}$$

The cosine function is

$$c\eta = \sqrt{1 - s^2\eta}\,\mathrm{SGN}[K_{31}\,s\upsilon_z + K_{32}\,c\upsilon_z)s\eta_x + K_{33}\,c\eta_x] \tag{E3}$$

There is no need to know the angle η explicitly; the trigonometric functions are sufficient.

The nominal υ_{zg} rotation about the sun line puts the x_p axis into the orbital plane, or

$$c_{12} = 0$$

which yields

$$K_{11}\,s\upsilon_{zg} + K_{12}\,c\upsilon_{zg} = K_{13}\,t\eta_x$$

or

$$s\upsilon_{zg} = \frac{K_{11}K_{13}\,t\eta_x - K_{12}\sqrt{(K_{11}^2 + K_{12}^2) - (K_{13}\,t\eta_x)^2}}{K_{11}^2 + K_{12}^2} \tag{E4}$$

$$c\upsilon_{zg} = \frac{K_{12}K_{13}\,t\eta_x + K_{11}\sqrt{(K_{11}^2 + K_{12}^2) - (K_{13}\,t\eta_x)^2}}{K_{11}^2 + K_{12}^2} \tag{E5}$$

The phase shift η_{tm} (midnight shift) of the cyclic gravity gradient torques (and consequently the shift of the resulting momenta) is the angle between the projection of the x_p axis into the orbital plane and the vehicle orbital x_{vo} axis, which yields

$$t\eta_{tm} = \frac{-c_{13}}{c_{11}}$$

or

$$\eta_{tm} = t^{-1}\left\{ \frac{-[(K_{11}\, s\upsilon_Z + K_{12}\, c\upsilon_Z)s\eta_X + K_{13}\, c\eta_X]}{K_{11}\, c\upsilon_Z - K_{12}\, s\upsilon_Z} \right\} \tag{E6}$$

APPENDIX F

MANEUVER MOMENTUM PREDICTION AND ADAPTIVE ANGLE COMMAND LIMITING

The maneuver commands of equations (21) and (22) are derived disregarding the fact that the CMG's may not have sufficient momentum available to execute the maneuvers. A prediction of the available maneuver momentum must be made at the time the onboard digital computer calculates the maneuver commands, which must be scaled down, if necessary, to avoid the introduction of severe crosscoupling.

The total CMG momentum $\underline{H}_t$ to be predicted can be split into a part $\underline{H}_g$ that is unalterable (momentum caused by cyclic components, the average, and the ramp) and a part $\underline{H}_{man}$ that can be changed (the momentum needed for the maneuvering itself and the momentum already desaturated by the maneuvers at the time in question):

$$\underline{H}_t = \underline{H}_g + \lambda \underline{H}_{man}$$

where λ is a positive number ($\lambda = 1$ indicates the unaltered case). The magnitude of this momentum is not allowed to exceed the saturation momentum H_{sat} of the CMG's:

$$(\underline{H}_g + \lambda \underline{H}_{man}) \cdot (\underline{H}_g + \lambda \underline{H}_{man}) = H_{sat}^2$$

or

$$\lambda = \left\{ -(\underline{H}_g \cdot \underline{H}_{man}) \pm \sqrt{(\underline{H}_g \cdot \underline{H}_{man})^2 + (\underline{H}_{man} \cdot \underline{H}_{man})[H_{sat}^2 - (\underline{H}_g \cdot \underline{H}_g)]} \Big/ (\underline{H}_{man} \cdot \underline{H}_{man}) \right\}$$

We can make the assumption that $H_{sat}^2 > (\underline{H}_g \cdot \underline{H}_g)$; i.e., without any maneuver the system is not saturated. Then only the plus sign in front of the square root results in a positive λ (a negative value for λ makes no sense; i.e., it indicates that a maneuver diametrically opposite to the one desired is necessary). When $\lambda > 1$, excess maneuver momentum is available and no scaling is necessary, whereas $\lambda < 1$ requires scaling.

The number of time points where the maneuver momentum is checked must be minimized and the halfway points for each of the three maneuvers and the point at the very end of the maneuvers (end of the desaturation interval) have been selected as the checkpoints. This is illustrated in Figure F1 which shows the orbital y and z components of the momenta, necessary for the maneuvering, added to the unalterable momentum, as a function of η_{td}. A different aspect of the same information is shown in Figure F2 where the z component is plotted as a function of the y component with η_{td} as a parameter. In this representation the saturation can be indicated as a circle about the origin in the y-z plane. The effect of an x momentum is also disregarded in Figures F1 and F2 (for clarity), but the equations do not neglect the x component. In the following the λ's carry a subscript identifying the checkpoints with which they are associated.

Saturation during the second maneuver is caused by a $\Delta\epsilon$ only and can be detected at checkpoint 2. It requires a reduction of the $\Delta\epsilon$'s by λ_2 if $\lambda_2 < 1$. Checkpoint 2 is at the maximum momentum (for the second maneuver), if there is no orbital y momentum to be desaturated, and close to it for the case depicted in Figure F1 (which has a large orbital y momentum). If saturation occurs at checkpoint 1 or 3, both the ϵ's and the $\Delta\epsilon$'s should be reduced proportionally by $\mathrm{MIN}(\lambda_1, \lambda_3)$ such that saturation is just reached at the respective checkpoint. After the checkpoints, the desired momentum still can exceed the available momentum. Some momentum is always available right after the first maneuver and attaining the exact attitude is not critical; therefore, it makes no difference if the available momentum is exceeded after its checkpoint. However, at the end of the third maneuver, the attitude error must be zero or experiment time will be lost. Figure F1 shows that enough excess momentum is always available between the start of the third maneuver and checkpoint 3 to meet the time integral of momentum required for the desired attitude change. Increasing the commanded rate initially by a factor of μ (which will be determined below) can be implemented by a fictitious reduction of the third maneuver interval by $\Delta\rho$. Figure F1 shows that the problem can be linearized (which is slightly conservative) and the relationships are shown in Figure F3, where the available maneuver momentum is normalized with respect to the desired maneuver command. The cyclic momentum has been subtracted, resulting in a sloped saturation line, and the polarity has been reversed for convenience. The momentum time integral requirement can be stated as (ρ is proportional to time)

$$\frac{\rho}{2}\mu - \frac{1}{2}\rho_1 (\mu - \lambda_4) = \frac{\rho}{2} \tag{F1}$$

where it should be remembered that the ordinate is normalized by the desired maneuver momentum. Geometric relationships show that

$$\rho_1 = \frac{\rho}{4} (\mu - \lambda_4)/(\lambda_3 - \lambda_4) \tag{F2}$$

Elimination of ρ_1 from equation (F1) yields

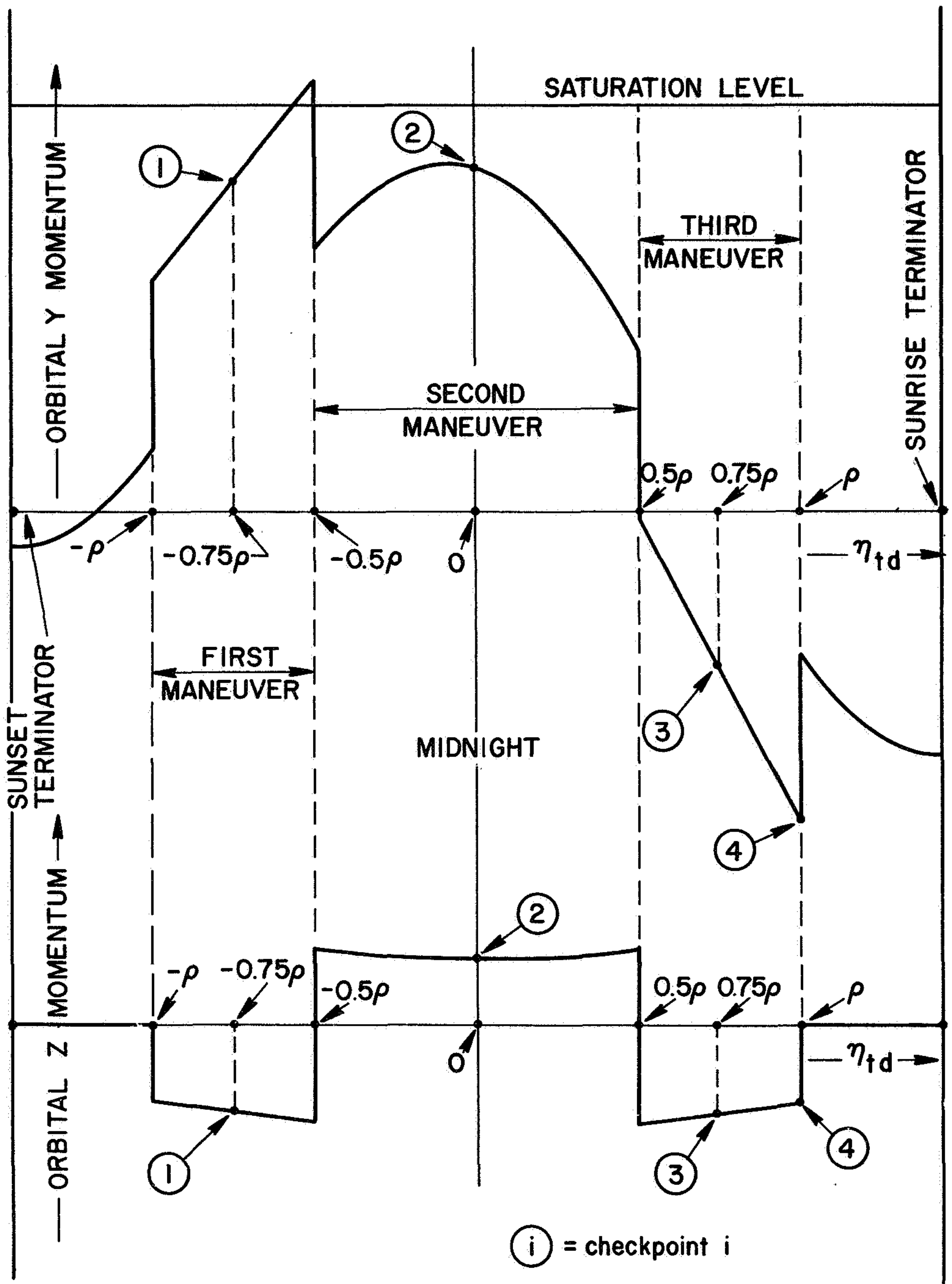

Figure F1. Checkpoints for maneuver momentum.

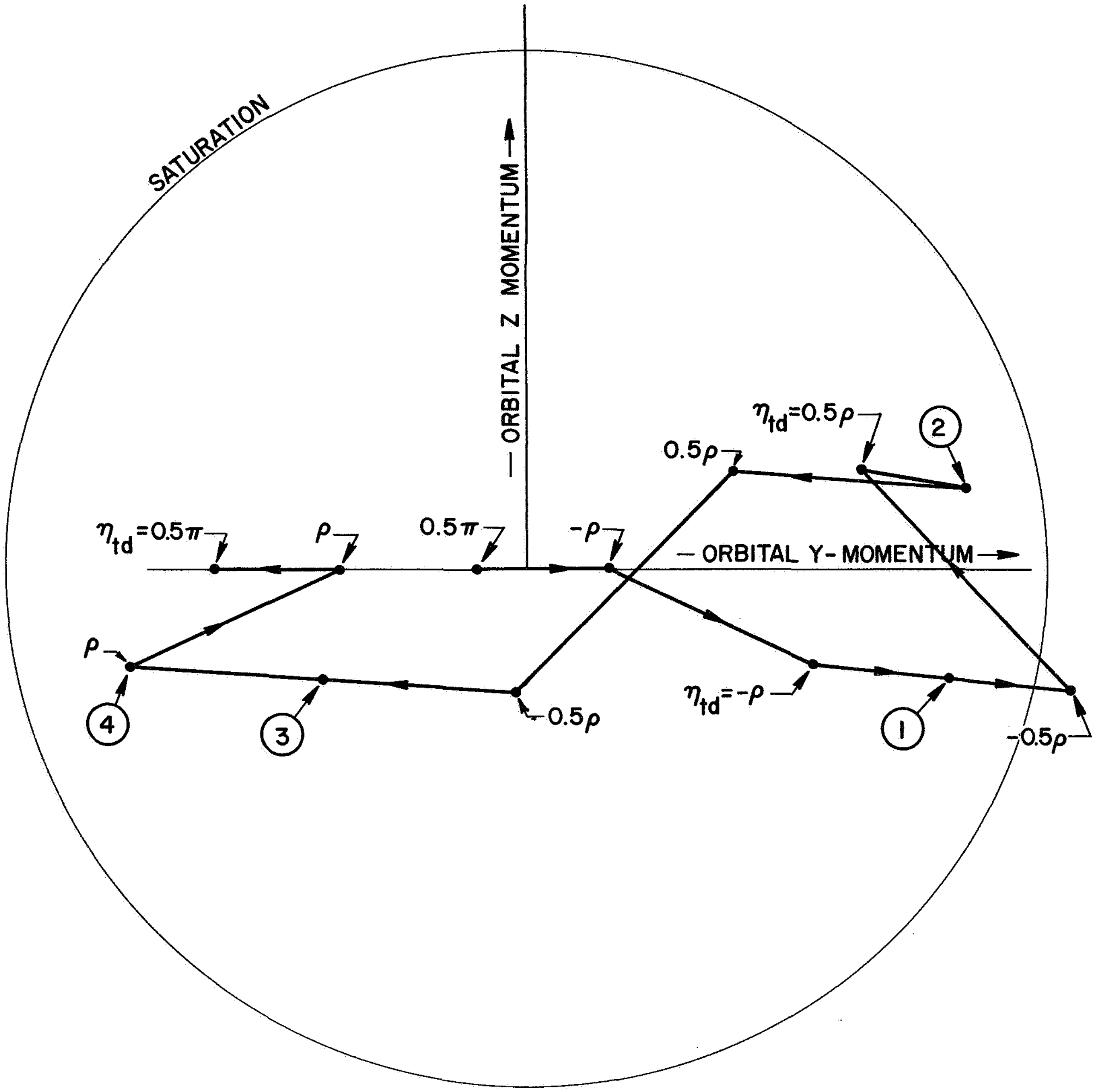

Figure F2. Orbital z versus orbital y momentum.

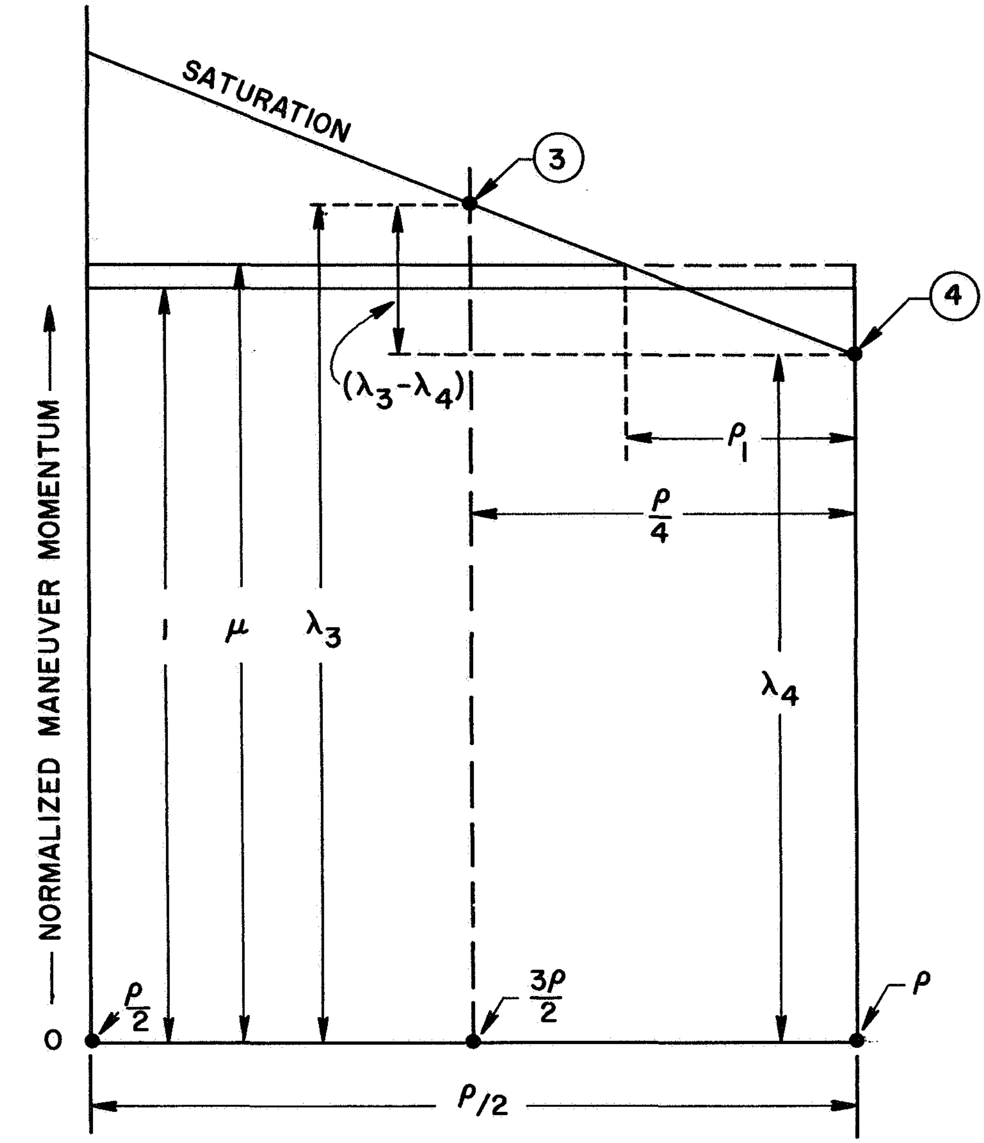

Figure F3. $\Delta\rho$-generation.

$$4(\mu - 1)(\lambda_3 - \lambda_4) - (\mu - \lambda_4)^2 = 0$$

$$\mu^2 - 2(2\lambda_3 - \lambda_4)\mu + \lambda_4 + 4(\lambda_3 - \lambda_4) = 0$$

or

$$\mu = (2\lambda_3 - \lambda_4) - 2\sqrt{(\lambda_3 - 1)(\lambda_3 - \lambda_4)} \tag{F3}$$

Only the minus sign before the square root makes sense. To achieve a velocity increase by a factor of μ by a shortening of the base by $\Delta\rho$ results in

$$\left[\left(\frac{\rho}{2}\right) - \Delta\rho\right]\mu = \frac{\rho}{2}$$

or

$$\Delta\rho = \left(1 - \frac{1}{\mu}\right)\left(\frac{\rho}{2}\right) \tag{F4}$$

A plot of $\Delta\rho/\rho$ is shown in Figure F4. A conservative approximation that eliminates the need for a square root is

$$\Delta\rho = \frac{1 - \lambda_4}{2\lambda_3 - \lambda_4}\left(\frac{\rho}{2}\right) \tag{F5}$$

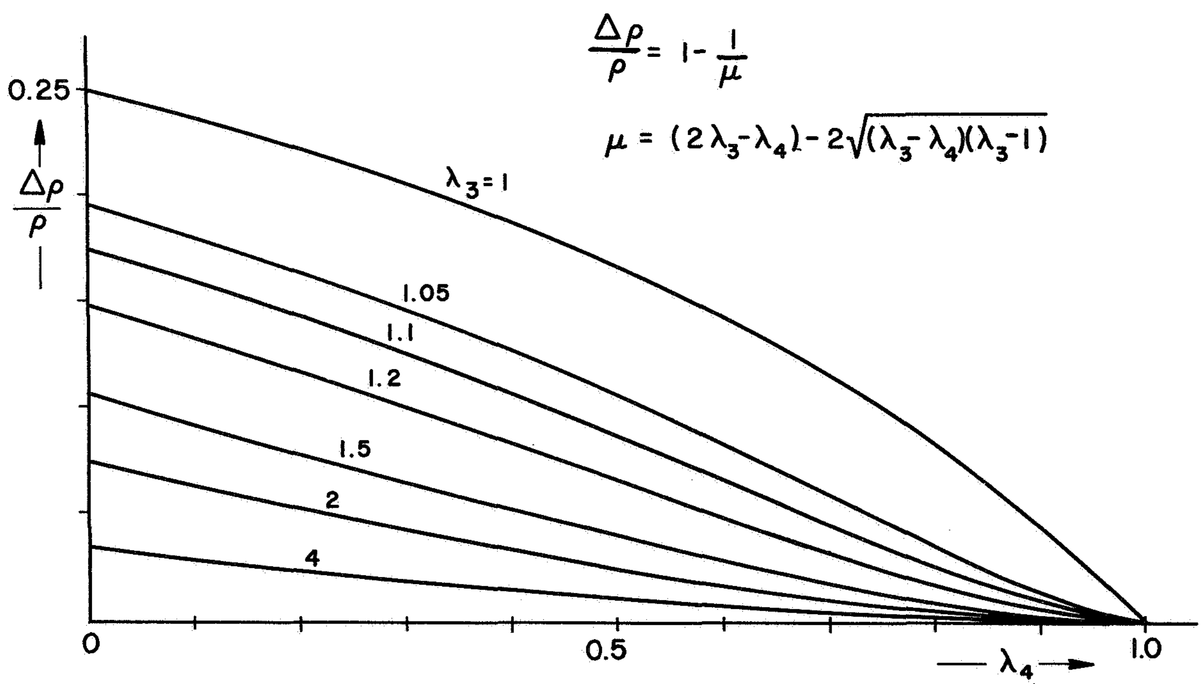

Figure F4. Exact $\Delta\rho/(\rho/2)$ versus λ_4.

A plot of $\Delta\rho/\rho$ for the approximation is shown in Figure F5. All objectives of the scaling can be cast into three equations [see equations (18), (21), and (22)]

$$\begin{bmatrix} \epsilon_{x1} \\ \epsilon_{y1} \\ \epsilon_{z1} \end{bmatrix} = \mathrm{MIN}(1, \lambda_1, \lambda_3) \begin{bmatrix} \epsilon_x \\ \epsilon_y \\ \epsilon_z \end{bmatrix} + \mathrm{MIN}(1, \lambda_1, \lambda_2, \lambda_3) \begin{bmatrix} \Delta\epsilon_x \\ \Delta\epsilon_y \\ \Delta\epsilon_z \end{bmatrix} \tag{F6}$$

$$\begin{bmatrix} \epsilon_{x2} \\ \epsilon_{y2} \\ \epsilon_{z2} \end{bmatrix} = \mathrm{MIN}(1, \lambda_1, \lambda_3) \begin{bmatrix} \epsilon_x \\ \epsilon_y \\ \epsilon_z \end{bmatrix} - \mathrm{MIN}(1, \lambda_1, \lambda_2, \lambda_3) \begin{bmatrix} \Delta\epsilon_x \\ \Delta\epsilon_y \\ \Delta\epsilon_z \end{bmatrix} \tag{F7}$$

$$\Delta v_z = -A_4\ \mathrm{MIN}(1, \lambda_3)\,(s\eta H_{dy} + c\eta H_{dz})/(2\pi c\eta_x) \tag{F8}$$

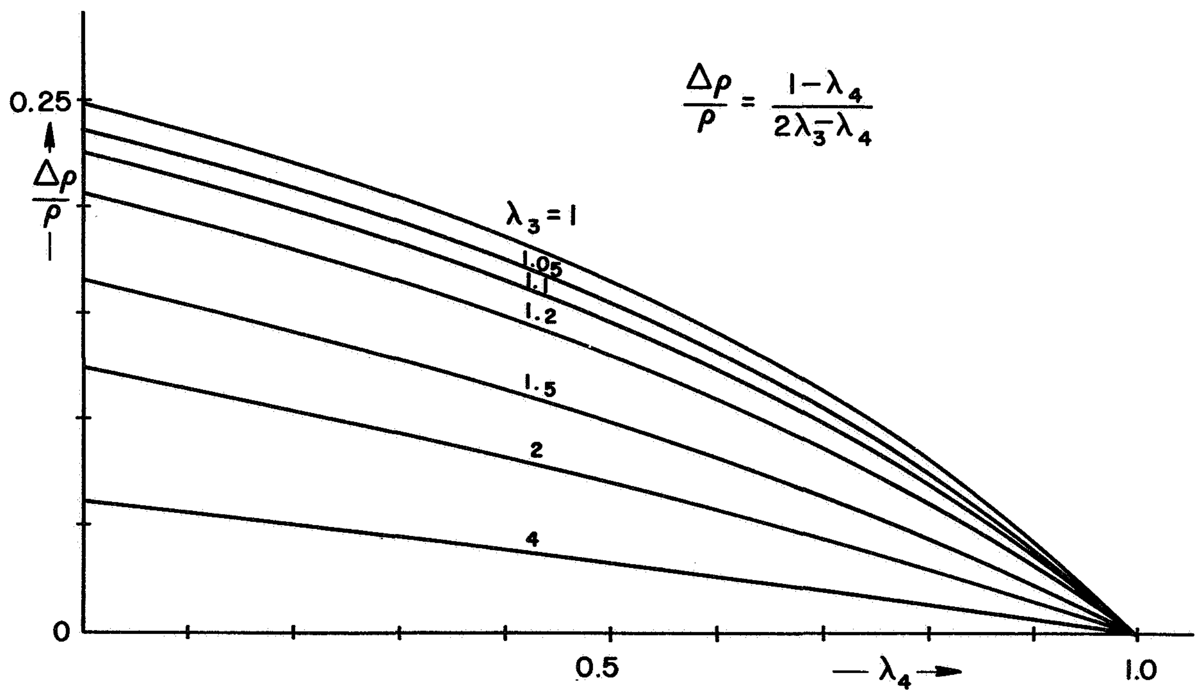

Figure F5. Approximate $\Delta\rho/(\rho/2)$ versus λ_4.

For each checkpoint there is a need to identify what constitutes the nonscalable vector $\underline{H}_{ni}$ and the scalable vector $\underline{H}_{sci}$. It is assumed that the components are in vehicle coordinates. In general [see equations (25), (G6), and (G7)],

$$\underline{H}_{ni} = \underline{H}_a + \underline{H}_b + K_{nki}\underline{H}_k + K_{gyi}\underline{H}_{gy} + K_{gzi}\underline{H}_{gz} + \underline{H}_{dni} \tag{F9}$$

where $\underline{H}_{dni}$ identifies the portion of the momentum already desaturated which is not affected by the particular λ_i. Also

$$\underline{H}_{sci} = -\frac{2\Omega}{\rho}\,[I]\,\underline{\epsilon}_i + \underline{H}_{dsi} \tag{F10}$$

where $\underline{\epsilon}_i$ signifies the change in angle during the maneuver in question and $\underline{H}_{dsi}$ is the portion of the already desaturated momentum which is affected by the particular λ_i.

The following constants apply to the momentum ramp $\underline{H}_k$:

$$K_{nk1} = 0.5 - 0.375\,\rho/\pi$$

$$K_{nk2} = 0.5$$

$$K_{nk3} = 0.5 + 0.375\,\rho/\pi$$

$$K_{nk4} = 0.5 + 0.5\,\rho/\pi$$

The following constants are associated with the cosine amplitude $\underline{H}_{gy}$ (or $\underline{H}_c$) and the sine amplitude $\underline{H}_{gz}$ (or $\underline{H}_s$) of the cyclic momenta [see equations (25), (G6), and (G7)]. Linearization was applied.

$$K_{gy1} = -1.5\,\rho + 0.5\,\pi$$

$$K_{gy2} = 1$$

$$K_{gy3} = -1.5\,\rho + 0.5\,\pi$$

$$K_{gy4} = -1.8\,\rho + 0.45\,\pi$$

$$K_{gz1} = -1$$

$$K_{gz2} = 0$$

$$K_{gz3} = +1$$

$$K_{gz4} = -1.7\,\rho + 0.85\,\pi$$

The desaturation momentum components must be in vehicle space, and the portion that will be desaturated by Δv_z after the desaturation interval (i.e., the orbital z momentum) must be subtracted:

$$\begin{bmatrix} H_{dvx} \\ H_{dvy} \\ H_{dvz} \end{bmatrix} = [K]^T \left\{ \begin{bmatrix} H_{dx} \\ H_{dy} \\ H_{dz} \end{bmatrix} - (s\eta H_{dy} + c\eta H_{dz}) \begin{bmatrix} 0 \\ s\eta \\ c\eta \end{bmatrix} \right. \qquad \text{(F11)}$$

The portion of the momentum that must be considered unscalable is

$$\underline{H}_{dn1} = [0, 0, 0]^T$$

$$\underline{H}_{dn2} = 0.5\,\mathrm{MIN}(1, \lambda_1, \lambda_3)\,[0, H_{dvy}, H_{dvz}]^T$$

$$\underline{H}_{dn3} = [0, 0, 0]^T$$

$$\underline{H}_{dn4} \quad \begin{bmatrix} \mathrm{MIN}(1, \lambda_1, \lambda_2, \lambda_3)\, H_{dvx} \\ \mathrm{MIN}(1, \lambda_1, \lambda_3)\, H_{dvy} \\ \mathrm{MIN}(1, \lambda_1, \lambda_3)\, H_{dvz} \end{bmatrix}$$

The portion of the desaturation momentum that can be scaled is

$$\underline{H}_{ds1} = [0, 0, 0]^T$$

$$\underline{H}_{ds2} = [0.5H_{dvx}, 0, 0]^T$$

$$\underline{H}_{ds3} = [H_{dvx}, H_{dvy}, H_{dvz}]^T$$

$$\underline{H}_{ds4} = [0, 0, 0]^T$$

The attitude changes during the maneuvers are

$$\underline{\epsilon}_1 = [\epsilon_{x1}, \epsilon_{y1}, \epsilon_{z1}]^T$$

$$\underline{\epsilon}_2 = [-\Delta\epsilon_x, -\Delta\epsilon_y, -\Delta\epsilon_z]^T$$

$$\underline{\epsilon}_3 = [-\epsilon_{x2}, -\epsilon_{y2}, -(\epsilon_{z2} - \Delta\upsilon_z)]^T$$

where equations (18), (19), and (20) supply the ϵ's and the $\Delta\epsilon$'s (i.e., the angles before scaling) but

$$\underline{\epsilon}_4 = [-\epsilon_{x2}, -\epsilon_{y2}, -(\epsilon_{z2} - \Delta\upsilon_z)]^T$$

where equations (F7) and (F8) supply the ϵ's and $\Delta\upsilon_z$ (i.e., the angles after scaling).

APPENDIX G

CYCLIC MOMENTUM COMPONENTS

The cyclic momentum components can be extracted from the samples [equation (23)]. However, in some cases one or more samples are invalid or missing, and an alternate way of determining the cyclic momentum components must be available.

The intended use is not critical, and it can be assumed that the large moments of inertia (about the y_p and z_p axes) are identical. This assumption allows a rotation about the x_p axis without a change in the gravity gradient torque vector. It is then convenient to develop the torque with the x_p axis out of the orbital plane by an angle υ_{ze} and with the z_p axis in the orbital plane:

$$\underline{T}_g = 3\Omega^2 \, \Delta I r_x \begin{bmatrix} 0 \\ -r_z \\ r_y \end{bmatrix}$$

with

$$\begin{bmatrix} r_x \\ r_y \\ r_z \end{bmatrix} = \begin{bmatrix} c\upsilon_{ze} & s\upsilon_{ze} & 0 \\ -s\upsilon_{ze} & c\upsilon_{ze} & 0 \\ 0 & 0 & 1 \end{bmatrix} \begin{bmatrix} c\eta_{td} & 0 & s\eta_{td} \\ 0 & 1 & 0 \\ -s\eta_{td} & 0 & c\eta_{td} \end{bmatrix} \begin{bmatrix} 0 \\ 0 \\ -1 \end{bmatrix}$$

$$= \begin{bmatrix} -c\upsilon_{ze} \; s\eta_{td} \\ s\upsilon_{ze} \; s\eta_{td} \\ -c\eta_{td} \end{bmatrix}$$

$$\Delta I = -(I_x - I_z) = I_y - I_x$$

or

$$\underline{T}_g = + \frac{3}{2} \Omega^2 \Delta I c\upsilon_{ze} \begin{bmatrix} 0 \\ -s2\eta_{td} \\ -s\upsilon_{ze}(1 - c2\eta_{td}) \end{bmatrix} \tag{G1}$$

Since we are only interested in the cyclic components, the bias in the z component can be ignored:

$$\underline{T}_{gc} = + \frac{3}{2} \Omega^2 \Delta I c\upsilon_{ze} \begin{bmatrix} 0 \\ -s2\eta_{td} \\ s\upsilon_{ze}\, c2\eta_{td} \end{bmatrix} \tag{G2}$$

Integration yields

$$\underline{H}_{gc} = \frac{3}{4} \Omega \Delta I c\upsilon_{ze} \begin{bmatrix} 0 \\ c2\eta_{td} \\ s\upsilon_{ze}\, s2\eta_{td} \end{bmatrix} \tag{G3}$$

where the average over one orbit has been set to zero. To be useful the cyclic momentum components should be in vehicle components:

$$\underline{H}_{gcv} = \frac{3}{4} \Omega \Delta I c\upsilon_{ze} [\upsilon_z] [\eta_x] [\eta_{tm}]^T [\upsilon_{ze}]^T \begin{bmatrix} 0 \\ c2\eta_{td} \\ s\upsilon_{ze}\, s2\eta_{td} \end{bmatrix} \tag{G4}$$

where η_{tm} is the angle about orbital y between the projection of the x_p axis into the orbital plane and the z_v axis into the orbital plane. Evaluation of equation (G4) yields

$$\underline{H}_{gvc} = \underline{H}_{gy}\, c2\eta_{td} + \underline{H}_{gz}\, s2\eta_{td} \tag{G5}$$

with

$$\underline{H}_{gy} = \frac{3}{4}\,\Omega\,\Delta I c\upsilon_{ze} \begin{bmatrix} -c\upsilon_z\, c\eta_{tm}\, s\upsilon_{ze} + s\upsilon_z\,(c\eta_x\, c\upsilon_{ze} + s\eta_x\, s\eta_{tm}\, s\upsilon_{ze}) \\ s\upsilon_z\, c\eta_{tm}\, s\upsilon_{ze} + c\upsilon_z\,(c\eta_x\, c\upsilon_{ze} + s\eta_x\, s\eta_{tm}\, s\upsilon_{ze}) \\ -s\eta_x\, c\upsilon_{ze} + c\eta_x\, s\eta_{tm}\, s\upsilon_{ze} \end{bmatrix} \tag{G6}$$

$$\underline{H}_{gz} = \frac{3}{8}\,\Omega\,\Delta I s2\upsilon_{ze} \begin{bmatrix} c\upsilon_z\, s\eta_{tm} + s\upsilon_z\, s\eta_x\, c\eta_{tm} \\ -s\upsilon_z\, s\eta_{tm} + c\upsilon_z\, s\eta_x\, c\eta_{tm} \\ c\eta_x\, c\eta_{tm} \end{bmatrix} \tag{G7}$$

Only the terms $s2\eta_{td}$ and $c2\eta_{td}$ must be updated frequently; the rest can be updated once per orbit. If υ_{ze} and η_{tm} can be considered small, equations (G6) and (G7) can be simplified to

$$\underline{H}_{gy} = \frac{3}{4}\,\Omega\Delta I \begin{bmatrix} -c\upsilon_z\, \upsilon_{ze} + s\upsilon_z\, c\eta_x \\ s\upsilon_z\, \upsilon_{ze} + c\upsilon_z\, c\eta_x \\ -s\eta_x \end{bmatrix} \tag{G8}$$

$$\underline{H}_{gz} = \frac{3}{4}\,\Omega\Delta I \begin{bmatrix} s\upsilon_z\, s\eta_x \\ c\upsilon_z\, s\eta_x \\ c\eta_x \end{bmatrix} \upsilon_{ze} \tag{G9}$$

An estimate must be made on υ_{ze}:

$$\upsilon_{ze} = (\upsilon_z - \upsilon_{zg})\, c\eta_x$$

where υ_{zg} is the z rotation needed to put the x_p axis into the orbital plane (see Appendix E for its derivation). Further simplification is possible if υ_{ze} can be considered negligible:

$$\underline{H}_{gy} = \frac{3}{4} \Omega \Delta I \begin{bmatrix} s\upsilon_z \, c\eta_x \\ c\upsilon_z \, c\eta_x \\ -s\eta_x \end{bmatrix} \tag{G10}$$

$$\underline{H}_{gz} = \begin{bmatrix} 0 \\ 0 \\ 0 \end{bmatrix} \tag{G11}$$

$\underline{H}_{gy}$ of equation (G10) is the resolution of a momentum along the orbital y axis into vehicle components.

APPENDIX H

SAMPLED DATA SYSTEM

The following equations are needed to treat the desaturation method as a sampled data system:

$$H_n = H_{n-1} + H_k + H_{dn-1} \tag{H1}$$

$$\Sigma H_n = \Sigma H_{n-1} + K_n H_n + K_{n-1} H_{n-1} \tag{H2}$$

$$H_{dn} = \Sigma H_n - H_k \tag{H3}$$

[see equations (28) and (29)] where H is the total accumulated momentum and $H_a = H$. H_k is the momentum accumulation per orbit.

Application of the z transform results in

$$h = z^{-1} h + h_k + z^{-1} h_d \tag{H4}$$

$$\Sigma h = z^{-1} \Sigma h + K_n h + z^{-1} K_{n-1} h \tag{H5}$$

$$h_d = \Sigma h - h_k \tag{H6}$$

or

$$\frac{h}{h_k} = \frac{(z-1)^2}{z^2 - (2 + K_n)z + (1 - K_{n-1})} \tag{H7}$$

The characteristic equation

$$z^2 - (2 + K_n)z + (1 - K_{n-1})$$

results in

$$z_{1,2} = 0.5[(2 + K_n) \pm \sqrt{(2 + K_n)^2 - 4(1 - K_{n-1})}] \tag{H8}$$

K_n is selected to be -1, which yields

$$z_{1,2} = 0.5 \pm \sqrt{K_{n-1} - 0.75}$$

This results in an oscillatory system for

$$K_{n-1} < 0.75$$

and the equivalent system[1] to equations (27) for

$$K_{n-1} = 1$$

since the $z = 1$ is cancelled by the numerator in H7.

1. Only true as long as no nonlinearities are encountered.

REFERENCES

1. Kennel, H. F.: Angular Momentum Desaturation for ATM Cluster Configuration Using Gravity Gradient Torques. NASA TM X-53748, May 27, 1968.

2. Chubb, W. B.; Schultz, D. N.; and Seltzer, S. M.: Attitude Control and Precision Pointing of the Apollo Telescope Mount. Journal of Spacecraft and Rockets, Vol. 5, No. 8, August 1968.

3. Chubb, W. B.: Stabilization and Control of the Apollo Telescope Mount. NASA TM X-53834, May 6, 1969.

4. Seltzer, S. M.: Developing an Attitude Control System for the Apollo Telescope Mount. (IEEE Transactions of the Second Asilomar Conference on Circuits and Systems, Pacific Grove, Calif., Paper No. 68-C-64-ASIL), October 30 - November 1, 1968.

5. Chubb, W. B.; and Seltzer, S. M.: Skylab Attitude and Pointing Control System. NASA TN D-6068, October 1970.

6. Singer, S. F.: Torques and Attitude Sensing in Earth Satellites. Academic Press, New York, 1964, p. 73.

7. Kennel, H. F.: Visualization of the Torque Caused by the Gravity Gradient Acting on a Space Vehicle of Arbitrary Moment of Inertia Distribution. NASA TM X-53786, July 16, 1968.

APPROVAL

ANGULAR MOMENTUM DESATURATION FOR SKYLAB USING GRAVITY GRADIENT TORQUES

By Hans F. Kennel

The information in this report has been reviewed for security classification. Review of any information concerning Department of Defense or Atomic Energy Commission Programs has been made by the MSFC Security Classification Officer. This report, in its entirety, has been determined to be unclassified.

This document has also been reviewed and approved for technical accuracy.

Hans H. Hosenthien

HANS H. HOSENTHIEN
Chief, R&D Analysis Office

F. B. Moore

F. B. MOORE
Director, Astrionics Laboratory

DISTRIBUTION

INTERNAL

DIR

DEP-T

AD-S
Dr. Stuhlinger

PD-DO
Dr. Thomason
Mr. Schultz
Mr. Nicaise

PM-AA
Mr. Ise
Mr. McDarris

PM-PR-M

PM-MO-O
Mr. Hall

PM-SE-ATM
Mr. Igou
Mr. Cagle
Mr. Keathley

PM-SL-EI
Mr. Hardy

I-MO-R
Mr. Golden

A&TS-MS-IL (8)

A&TS-MS-IP (2)

A&TS-MS-H

A&TS-PAT
Mr. Wofford

A&TS-TU (15)
Mr. Winslow

S&E-DIR
Mr. Richard

S&E-CSE-DIR
Dr. Haeussermann
Mr. Mack

S&E-CSE-I
Mr. Blackstone

S&E-CSE-M
Mr. Marmann
Mr. Tinius

S&E-CSE-F
Mr. Wiesenmaier

S&E-CSE-A
Mr. Hagood

S&E-AERO-DIR
Dr. Geissler
Mr. Horn

S&E-AERO-D
Mr. Ryan
Dr. Worley (5)
Mr. Rheinfurth (2)

S&E-ASTN-SMA
Mr. Larson

S&E-COMP-S
Dr. Polstorff (5)

S&E-QUAL-PFN
Mr. Harne
Mr. Mitchell

DISTRIBUTION (Continued)

INTERNAL (Concluded)

S&E-ASTR-DIR
- Mr. Moore
- Mr. Horton

S&E-ASTR-A
- Mr. Hosenthien
- Dr. Seltzer
- Dr. Borelli
- Dr. Nurre
- Mr. Jones
- Mr. Kennel (50)
- Miss Flowers

S&E-ASTR-C
- Mr. Swearingen
- Mr. Lewis
- Mr. Coppock
- Mr. Hall
- Mr. Bridges
- Mr. Garrett
- Mr. Richards
- Mr. Owens
- Mr. Beckham (8)

S&E-ASTR-G
- Mr. Mandel
- Dr. Doane
- Mr. Jones
- Mr. Kalange
- Mr. Smith
- Mr. Howard

S&E-ASTR-BA
- Mr. Rowell

S&E-ASTR-S
- Mr. Wojtalik
- Mr. Gilino
- Mr. Noel
- Mr. Brooks
- Mr. Blanton
- Mr. Thompson
- Mr. Rupp
- Mr. Chubb (5)
- Mr. Applegate
- Mr. Polites
- Mr. Davis
- Mr. Fisher (3)
- Mr. Scott (2)
- Mr. Scofield
- Mr. Shelton (5)
- Mr. Hahn (Bendix) (5)
- Mr. Sloan (Sperry)
- Mr Faison (Sperry) (5)

S&E-ASTR-ZX

EXTERNAL

NASA-HQ-MLO
- Mr. Hamby

NASA-HQ-MLS (Bellcom)
- Mr. Kranton
- Mr. Corey
- Mr. DeGraaf (2)

NASA-MSC-FC5
- Mr. Parker (20)

NASA-MSC-KM
- Mr. Tindall

DISTRIBUTION (Continued)

EXTERNAL (Continued)

NASA-MSC-FS5
Mr. Clayton

NASA-MSC-FM4
Mr. Blucker

NASA-MSC-MIT/SDL
Mr. Stubbs
Mr. Turnbull
Mr. David
Mr. Millard
Mr. Greene
Mr. Hoag

NASA-MSC-CF-413 (MDAC)
Mr. Glowczwski

NASA-KSC-AA-SVO-3
Mr. Bland (4)

NASA-KSC-LC-ENG-61
Mr. Klaus

NASA-LRC
Dr. Kurzhals (5)

International Business Machines (10)
150 Sparkman Dr.
Huntsville, Ala. 35805
Attn: Mr. McPherson, Dept. 207

Lockheed Missiles and Space Co. (3)
4800 Bradford Dr.
Huntsville, Ala. 35805
Attn: Mr. Heeschen, Dept. 5430

McDonnell Douglas Astronautics Co. (3)
Rm. 41, Bldg. 4481
Marshall Space Flight Center, Ala. 35812
Attn: Mr. Roth/Mr. Williams

McDonnell Douglas Aircraft Co. (2)
Huntington Beach, Calif.
Attn: Mr. Rabinoff, A3/253
Mr. Schar, 8A3/253/AZC2

Thompson-Ramo-Wooldridge Co. (2)
1710 Festival Dr.
Houston, Tex. 77058
Attn: Mr. Stephens/Mr. Chao

Naval Research Laboratories
Washington, D. C. 20390
Attn: Mr. Schumacher, ATM Program
Manager Code 7149

Martin Marietta Co.
P. O. Box 3040
Huntsville, Ala. 35810
Attn: Mr. Harmon

NASA-KSC-FCDS-Cape
Attn: Mr. Hughes

Martin Marietta Corp., Denver Div. (5)
P. O. Box 179
Denver, Colo. 80201
Attn: Mr. Kraft/Mr. Glahn (4)

McDonnell Douglas Astr. Co.
16915 Elcamino Rd., Suite 220
Houston, Tex. 77058
Attn: Mr. Boatman, -ED

Bendix Research Laboratories (2)
10 1/2 Mile Rd.
Southfield, Mich. 48075
Attn: Mr. B. K. Powell

DISTRIBUTION (Concluded)

EXTERNAL (Concluded)

Bendix Research Laboratories (5)
2796 S. Federal Blvd.
Denver, Colo. 80236
Attn: Mr. Duncan

Bendix Corp. Nav. & Contr. Div. (9)
Teterboro, N. J. 07608
Attn: Mr. Morine, Dept. 7511

Scientific and Technical Information Facility (25)
P. O. Box 33
College Park, Md. 20740
Attn: NASA Repr. (S-AK/RKT)

University of California
School of Engineering and Applied Science
Mechanics and Structure Dept.
Los Angeles, Calif. 90024
Attn: Mr. D. L. Mingori